Old Dominion University
ODU Digital Commons

Mechanical & Aerospace Engineering Theses & Dissertations | Mechanical & Aerospace Engineering

Winter 1996

Application of Reanalysis Techniques for Pattern Design of Spot Welds

Young San Kim
Old Dominion University

Follow this and additional works at: https://digitalcommons.odu.edu/mae_etds

Part of the Automotive Engineering Commons, and the Mechanical Engineering Commons

Recommended Citation
Kim, Young S.. "Application of Reanalysis Techniques for Pattern Design of Spot Welds" (1996). Doctor of Philosophy (PhD), Dissertation, Mechanical & Aerospace Engineering, Old Dominion University, DOI: 10.25777/9as2-5324
https://digitalcommons.odu.edu/mae_etds/147

This Dissertation is brought to you for free and open access by the Mechanical & Aerospace Engineering at ODU Digital Commons. It has been accepted for inclusion in Mechanical & Aerospace Engineering Theses & Dissertations by an authorized administrator of ODU Digital Commons. For more information, please contact digitalcommons@odu.edu.

APPLICATION OF REANALYSIS TECHNIQUES FOR PATTERN DESIGN OF SPOT WELDS

by

Young San Kim

A Dissertation Submitted to the Faculty of Old Dominion University in Partial Fulfillment of the Requirements for the Degree of

DOCTOR OF PHILOSOPHY

in

MECHANICAL ENGINEERING

OLD DOMINION UNIVERSITY
December 1996

Approved by:

Gene Hou, Director

Chuh Mei

Stephen G. Cupschalk

Jen-Kuang Huang

Reproduced with permission of the copyright owner. Further reproduction prohibited without permission.

ABSTRACT

APPLICATION OF REANALYSIS TECHNIQUES
FOR PATTERN DESIGN OF SPOT WELDS.

Young San Kim
Old Dominion University, 1996
Director: Dr. Gene Hou

Extensive benchmarking on competitive cars has shown that the durability of vehicles, assembly-induced variations, and assembly cost are directly related to the quality and number of spot welds. On most luxury cars, approximately 4,500 to 5,000 spot welds are found. On less expensive cars, the range is from 3,500 to 4,500. These cars usually inherit more noise, rattles, squeaks, and other quality-related problems. These problems have motivated the search for a new capability to systematically place welds in the most critical areas, with a minimum number of welds for car bodies, while satisfying all performance requirements (e.g., stiffness, stress distribution, load paths, and durability). This research represents an initial attempt to develop this aforementioned capability.

The main thrust of the research is to develop the framework for a numerical approach for optimal pattern design of spot welds and to assess the applicability of the approach in an industrial environment.

The pattern design of spot welds in this study is viewed as a combinatory design optimization problem and is solved by a genetic-algorithm-based search method incorporated with an efficient reanalysis technique. The reanalysis technique models the spot welds as multiple-point constraints and uses the Sherman-Morrison identity to recursively calculate the new solution of the structure subjected to modification on

Reproduced with permission of the copyright owner. Further reproduction prohibited without permission.

the joint and support conditions. This optimization procedure is verified with several numerical examples. The results show that the proposed optimization procedure is effective and can be extended to realistic applications for pattern design of spot welds.

Reproduced with permission of the copyright owner. Further reproduction prohibited without permission.

ACKNOWLEDGMENTS

I would like to express my sincere appreciation to my advisor, Dr. Gene Hou, for his advice and help during this study. I am also grateful to Drs. Chuh Mei, Stephen G. Cupschalk, and Jen-Kuang Huang for their many suggestions and valuable advice. I would also like to extend my thanks to Drs. Surendra N. Tiwari, Robert L. Ash, and Sushil Chaturvedi for their helps during my study.

I would like to thank the families of Mr. Jae Min Kim and Dr. Han Jun Woo for their encouragement and assistance throughout my long association with them.

I am deeply grateful to my parents, who have been a constant source of encouragement, support, and inspiration throughout my studies. I would like to thank my sisters and brothers-in-law for their help during my difficult times. Finally, without my son, I would not have finished this work.

This study was partially supported by the Department of Mechanical Engineering at Old Dominion University.

Reproduced with permission of the copyright owner. Further reproduction prohibited without permission.

TABLE OF CONTENTS

Reproduced with permission of the copyright owner. Further reproduction prohibited without permission.

Reproduced with permission of the copyright owner. Further reproduction prohibited without permission.

LIST OF SYMBOLS

a_i	Measurement of state of stresses in spot weld i
a_o	Desired bound of state of stresses in spot welds
a_{ji}	Mathematical notation of A
A	Eigenvector expansion matrix
$\mathbf{b}$	Averaged bandwith of stiffness matrix
b	Design variable
$\mathbf{c}$	Constant vector
c_j	Mathematical notation of $\mathbf{c}$
C	Compliance of structure
C_o	Desired bound of compliance of welded structure
D	Diagonal matrix made of ν_i
E_i	Eigenvectors of ΔK
$\mathbf{f}$	Load vector
$\mathbf{f}_0$	Load vector of existing structure
F	Composite function representing objective
g	Inequality constraints
h	Equality constraints
I	Identity matrix
K	Stiffness matrix
$\overline{K}$	Augmented stiffness matrix

Reproduced with permission of the copyright owner. Further reproduction prohibited without permission.

ΔK	Changes in stiffness matrix
m	Total number of degrees of freedom at spot welds
n	Dimension of structure without spot welds
N	Number of operations
N_a	Node of member A
N_b	Node of member B
N	Number of spot welds
p	Number of new patterns
Q	Value of $K^{-1}V$
Q_i	Value of $K^{-1}E_i$
r	Denominating factor for normalizing
r'	Penalty coefficient
R	Reaction force at constraint
s	Denominating factor for normalizing
s'	Penalty coefficient
S	Violation of stress constraints
$\mathbf{u}_i$	Unit forces applied at constrained points
$\mathbf{u}_{i,a}$	Subset of $\mathbf{u}_i$ that relates to node N_a only
$\mathbf{u}_{i,b}$	Subset of $\mathbf{u}_i$ that relates to node N_b only
u	Displacement in x direction under original force
u'	Displacement in x direction due to unit reaction force
U	Unit matrix that corresponds to single-point constraint
v	Displacement in y direction under original force
V	Matrix made of E_i

Reproduced with permission of the copyright owner. Further reproduction prohibited without permission.

VDV^T	Modification factor of K
w	Displacement in z direction under original force
w'	Displacement in z direction due to unit reaction force
W	Violation of compliance constraint
VW^T	Modification factor of K
$\mathbf{x}$	Displacement vector of modified structure
$\mathbf{x_1}$	Displacement due to unit force
$\mathbf{x_0}$	Displacement vector of existing structure
$\mathbf{x_a}$	Displacement vector at node N_a
$\mathbf{x_b}$	Displacement vector at node N_b
$\mathbf{x_i}$	Set of displacements due to unit forces
$\mathbf{x_{i,a}}$	Subset of $\mathbf{x_i}$ that relates to node N_a only
$\mathbf{x_{i,b}}$	Subset of $\mathbf{x_i}$ that relates to node N_b only
xy^T	Modification factor of K
x_i	Mathematical notation of $\mathbf{x}$
α	Weighting coefficient
β	Weighting coefficient
γ	Weighting coefficient
λ	Lagrange multipliers associated with multiple-point constraint
ν_i	Eigenvalues of ΔK
θ_x	Rotation in x direction under original force
θ_y	Rotation in y direction under original force
θ_z	Rotation in z direction under original force
Ψ	Single-valued merit function

Reproduced with permission of the copyright owner. Further reproduction prohibited without permission.

Subscripts:

1, 2	Pair indices
a, b	Structural parts indices
i, j	Component indices

Superscripts:

T	Matrix transpose
-1	Matrix inverse

Reproduced with permission of the copyright owner. Further reproduction prohibited without permission.

LIST OF TABLES

Reproduced with permission of the copyright owner. Further reproduction prohibited without permission.

LIST OF FIGURES

Reproduced with permission of the copyright owner. Further reproduction prohibited without permission.

Reproduced with permission of the copyright owner. Further reproduction prohibited without permission.

CHAPTER 1

INTRODUCTION

1.1 Motivation and Objectives

Spot welding is a common manufacturing process in the automobile industry used in the assembly of vehicle body parts. In this process, the parts to be welded are placed on a specially designed floor jig and held together with clamps before welding. The quality of the welded product depends upon the initial gaps between the parts, the pattern of the spot welds, the welding sequence, and the quality of the spot-welding process. Extensive benchmarking on competitive cars has shown that the durability of vehicles, assembly-induced variations, and assembly cost are directly related to the quality and number of spot welds. On most luxury cars, approximately 4,500 to 5,000 spot welds are found. On less expensive cars, the range is from 3,500 to 4,500. These cars usually inherit more noise, rattles, squeaks, and other quality-related problems.

Table 1.1 summarizes a survey of 13 domestic and imported cars marketed between 1990 and 1995. The numbers of body parts and spot welds in domestic cars are generally less than those in imported ones, which reflects the difference in design policies; domestic-car design emphasizes a reduction in the number of pieces and in die and tooling costs, whereas imported-car design emphasizes the increase in the structural and manufacturing flexibility.

In acknowledgment of the importance of spot welds, several research efforts have been undertaken to study the spot-welding process and modeling; however, a systematic and numerically oriented approach has not yet been established to aid in design and manufacturing processes. The development and implementation of

Reproduced with permission of the copyright owner. Further reproduction prohibited without permission.

such an approach is, thus, an ultimate goal for many engineers and researchers in the automobile industry. The research reported here represents an initial attempt in reaching this goal.

Table 1.1. Survey of 13 Model Cars for Body Parts and Spot Welds

Domestic cars: 1990–1995			Imported cars: 1990–1995		
Car no.	No. of body parts	No. of spot welds	Car no.	No. of body parts	No. of spot welds
1	290	3320	1	410	4300
2	300	4070	2	430	3940
3	310	3300	3	440	4900
4	320	4620	4	450	3930
5	320	3980	5	460	4290
6	340	3550	6	470	4590
7	390	4490	-	-	-
Ave.	320	3904	Ave.	443	4325

The main thrust of this research is, therefore, to develop a framework for a methodology for the optimal pattern design of spot welds. The specific issues to be studied are listed below:

1. To derive a design formulation for measuring the performance of different patterns of spot welds in terms of structural integrity and manufacturability.
2. To develop an efficient reanalysis technique for analyzing structures with different spot weld patterns. It is understand that a spot weld can be modeled as a multiple-point constraint(MPC), a rigid element, or a flexible beam.
3. To develop an efficient design methodology for optimal patterning of spot welds under modification of joint and support conditions.

Reproduced with permission of the copyright owner. Further reproduction prohibited without permission.

In order to facilitate the implementation and validation of the proposed method, several sample problems in spot welding are investigated later in this study.

1.2 Scope of the Study

A methodology that combines an efficient reanalysis technique and a genetic algorithm is proposed here to optimally determine the required number of spot welds between a pair of assembled automotive components, as well as the locations of the spot welds. The genetic algorithm is used to deal with the discrete nature of the variables in the pattern design of spot welds; the efficient reanalysis technique is used to reduce the computational cost for repetitively analyzing the modified structure. This reduction in cost is necessary in order to apply this methodology to a large-scale, realistic problem.

Similar to a sensitivity analysis, the efficient reanalysis technique takes advantage of the fact that the stiffness matrix of the original structure has been factorized; thus, the technique uses only forward and backward substitution for quick analysis. Note, though, that the efficient reanalysis technique is different from sensitivity analysis in that the former will give an exact calculation of the perturbed design subjected to finite modifications and the latter will give only an approximate calculation. Finite modifications in this study pertain to the addition and the removal of spot welds.

The genetic algorithm selected for use here is a random search algorithm that follows Darwin's survival law to determine a set of better designs from iteration to iteration. Unlike the algorithms that are commonly used in engineering optimization techniques, the genetic algorithm does not need gradient information to determine the search direction. As a result, the genetic algorithm can conveniently handle discrete design variables. Furthermore, the random nature of the genetic algorithm has been proved to be able to locate the global minimum of the design problem. With these attractive features, the genetic algorithm has recently gained popularity among

Reproduced with permission of the copyright owner. Further reproduction prohibited without permission.

researchers and designers in design optimization. Nevertheless, the genetic algorithm becomes highly effective only when the analysis code does not require a great deal of computational time.

The rest of the chapters are organized as follows. Chapters 2, 3, and 4 discuss the proposed reanalysis technique for analyzing a structure; linear constraints are added or removed. The derivation of the basic equation for structural reanalysis is given in chapter 2. The procedure for using such an equation for reanalyzing structures with a modified constraint condition is given in chapter 3 and this procedure is demonstrated by numerical example in chapter 4. Chapter 5 presents the proposed methodology for optimum spot-weld patterning. Several sample problems are included in chapter 5 for verification. Concluding remarks are given in chapter 6.

1.3 Literature Review

Spot welding is an industrial application of interface methods that connect component members together. Mathematically, a spot weld represents a set of equality constraints that require the displacements of joining members at the spot weld to be the same. Therefore, spot welding can be formulated and analyzed by using the methods of tearing and interconnecting [1,2]. One group of these methods uses the theorem of Lagrange multipliers to form an augmented system equation that includes the Lagrange multipliers as unknowns to account for the equality constraints in modeling the interface conditions. Much of the recent work on structural tearing and interconnecting focuses either on discretization of the continuous interface conditions [3–5] or on improvement of computational efficiency by parallelization [6]. Moreover, those works emphasize only the interconnecting portion of the analysis, in which the structure members are connected together; these works do not address problems for tearing structural members apart. (Here, tearing implies the removal of the interface constraints from the involved structures.)

Reproduced with permission of the copyright owner. Further reproduction prohibited without permission.

Another group of methods that can be extended to structural tearing and interconnecting are the methods for structural modification. The structural modifications referred to here include the addition and removal of structural members from the structures. These methods efficiently reanalyze the modified structures without explicitly introducing the Lagrange multipliers. Generally speaking, these methods can be categorized into three groups: those based on the initial strain or initial stress concept [7–9], those based on the concept of parallel elements [10,11], and those based on algebraic approaches [12–14].

The application of the initial strain concept for structural modifications is not a new concept [7]. However, Argyris and Kelsey [8] are the first to present it in matrix notation. In their early work, initial strains are introduced to the cut-out member so that no internal forces are exerted from the cut-out element to the remaining structure. More recently, the initial strain concept has been extended to more general applications [9].

In the concept of parallel elements, a structural modification is modeled as an element attached in parallel to the element member that is to be modified [10]. The stiffness of the parallel element is equal to the change in the stiffness of the modified member. The forces of interaction between the parallel element and the member to be modified can then be calculated based on the compatibility and equilibrium conditions. The response of the modified structure obtained is that of the original structure subjected to the interaction and original external forces. The concept of parallel elements has been extended to shape optimization recently in Ref. 11, in which the stiffness of boundary elements is subjected to modification as a result of the change of boundary shape.

The fundamental equation used in the algebraic approach is the Sherman-Morrison equation [15]. To use the Sherman-Morrison equation, modifications of the stiffness

Reproduced with permission of the copyright owner. Further reproduction prohibited without permission.

matrix must be represented in the form of vector products. The Sherman-Morrison equation can then be used to calculate the exact inversion of the modified stiffness matrix in terms of the inversion of the original stiffness matrix. Various forms of the Sherman-Morrison equation have been developed in the past for structural reanalysis [12–14].

In this study, the Sherman-Morrison equation is modified and applied for fast reanalysis of various patterns of spot welds. In the equation, the original stiffness matrix is associated with the structures with no spot welds, and the matrix modification is associated with Lagrange multipliers, which represent constraint sets for spot welds. The matrix modification is changed for different patterns of spot welds, and the constraint set is changed if the pattern of spot welds is changed.

Reproduced with permission of the copyright owner. Further reproduction prohibited without permission.

CHAPTER 2

MODIFIED SHERMAN-MORRISON IDENTITY

This chapter lays out the theoretical foundation for the development of the modified Sherman-Morrison identity that is used in the later part of this dissertation for efficient structural reanalysis.

The original Sherman-Morrison identity is given as

$$\left(K + xy^T\right)^{-1} = K^{-1} - K^{-1}x\left(1 + y^T K^{-1} x\right)^{-1} y^T K^{-1} \tag{2.1}$$

where xy^T represents modification of K. Moreover, Eq.(2.1) can be extended to more general modifications as

$$\left(K + VW^T\right)^{-1} = K^{-1} - K^{-1}V\left(I + W^T K^{-1} V\right)^{-1} W^T K^{-1} \tag{2.2}$$

In this study, the Sherman-Morrison identity is generalized as

$$\left(K + VDV^T\right)^{-1} = K^{-1} - K^{-1}VD\left(I + V^T K^{-1} VD\right)^{-1} V^T K^{-1} \tag{2.3}$$

which considers the modification of K to be VDV^T, where V and D are matrices of dimension $n \times m$ and $m \times m$, respectively. If the dimension of m is much smaller than n, then the above equation provides an efficient method for determining the solution of the modified matrix equation.

To prove Eq.(2.3), we begin with the following equation:

$$\left(K + VDV^T\right)\mathbf{x} = \mathbf{f} \tag{2.4}$$

By premultiplying the above equation with K^{-1}, we obtain

$$\left(I + K^{-1}VDV^T\right)\mathbf{x} = K^{-1}\mathbf{f} \tag{2.5}$$

Reproduced with permission of the copyright owner. Further reproduction prohibited without permission.

which gives

$$\mathbf{x} + K^{-1}VD\left(V^T\mathbf{x}\right) = \mathbf{x_0} \tag{2.6}$$

where $\mathbf{x_0}$ is the solution of the original matrix (i.e., $K\mathbf{x_0} = \mathbf{f}$). By premultiplying V^T with Eq.(2.6) again, one has

$$\left(V^T\mathbf{x}\right) + V^TK^{-1}VD\left(V^T\mathbf{x}\right) = V^T\mathbf{x_0} \tag{2.7}$$

or

$$V^T\mathbf{x} = \left(I + V^TK^{-1}VD\right)^{-1}V^T\mathbf{x_0} \tag{2.8}$$

Note that the dimension of I in the above equation is $m \times m$. Equation (2.6) can then be rewritten as

$$\mathbf{x} = \mathbf{x_0} - K^{-1}VD\left(I + V^TK^{-1}VD\right)^{-1}V^T\mathbf{x_0} \tag{2.9}$$

which yields Eq.(2.3). Note that $K^{-1}V$ can be obtained as the solution Q of the following equation:

$$KQ = V \tag{2.10}$$

As K has been assembled and factorized when $\mathbf{x_0}$ is solved, the solution of Eq.(2.10) can be found with m backward substitutions. Any matrix modification ΔK can be decomposed by singular value decomposition [15] as

$$\Delta K = VDV^T \tag{2.11}$$

where D is a diagonal matrix with nonzero singular values of ΔK. Therefore, at least theoretically, Eq.(2.9) can be used for efficient reanalysis of a structure under any modification represented by ΔK. This proposed reanalysis technique can be implemented with any commercially rated finite-element analysis code (e.g., MSC/NASTRAN).

Reproduced with permission of the copyright owner. Further reproduction prohibited without permission.

CHAPTER 3

REANALYSIS TECHNIQUES FOR MODIFICATION OF STRUCTURAL SUPPORT CONDITIONS

Many connections and fasteners used in structural assembly can be modeled as single-point constraints (SPC's) or multiple-point constraints (MPC's), which involve only 1 or more than 1 degree of freedom, respectively. In this chapter, an efficient computational procedure is presented to analyze structures for which support conditions are under modification.

3.1 Introduction

An MPC is a linear constraint that involves more than 1 degree of freedom. Mathematically, this constraint can be written as

$$\sum_{i=1}^{n} a_{ji}x_i = c_j, \quad j = 1 \text{ through } p \tag{3.1}$$

or in matrix form as

$$A\mathbf{x} = \mathbf{c} \tag{3.2}$$

where A is a $p \times n$ rectangular matrix and $\mathbf{c}$ is a constant vector.

A spot weld is a typical example of an MPC in practice. The purpose of a spot weld is to join several metal sheets together at a single point. A method for modeling the characteristics of the welded metal has not yet been determined. In practice, the spot weld is usually modeled as a rigid bar or as a stiffened beam that connects the metal sheets. Mathematically, spot welds can be viewed as an interface condition,

Reproduced with permission of the copyright owner. Further reproduction prohibited without permission.

where two structural parts are joined together at discrete points. The compatibility condition requires that the displacements at the spot welds be equal. That is,

$$\mathbf{x}_{\mathrm{a}} = \mathbf{x}_{\mathrm{b}} \tag{3.3}$$

for a spot weld that joins nodes $\mathrm{N_a}$ and $\mathrm{N_b}$, where $\mathbf{x}_{\mathrm{a}}$ and $\mathbf{x}_{\mathrm{b}}$ are the displacement vectors at nodes $\mathrm{N_a}$ and $\mathrm{N_b}$, respectively. Specifically, the set of six compatibility conditions in Eq.(3.3) can be represented by MPC as follows:

$$\begin{aligned} u_{\mathrm{a}} &= u_{\mathrm{b}} \\ v_{\mathrm{a}} &= v_{\mathrm{b}} \\ w_{\mathrm{a}} &= w_{\mathrm{b}} \\ \theta_{x,\mathrm{a}} &= \theta_{x,\mathrm{b}} \\ \theta_{y,\mathrm{a}} &= \theta_{y,\mathrm{b}} \\ \theta_{z,\mathrm{a}} &= \theta_{z,\mathrm{b}} \end{aligned} \tag{3.4}$$

The MPC described above can then be conveniently rewritten in the form of Eq.(3.2), where A is a $6 \times n$ matrix and $\mathbf{x}$ is the $n \times 1$ displacement vector of the structure. However, most of the entries in A are zero, except those degrees of freedom that are associated with nodes $\mathrm{N_a}$ and $\mathrm{N_b}$. More specifically, A can be expressed as

$$A = [0\,0\,0 \ldots 0\, I\, 0\,0 \ldots 0\; -I\, 0\,0] \tag{3.5}$$

where $[0]$ is a 6×6 null matrix and $[I]$ and $[-I]$ are positive and negative 6×6 identity matrices that correspond to the degrees of freedom associated with nodes $\mathrm{N_a}$ and $\mathrm{N_b}$.

In the context of theory of Lagrange multipliers, Eq.(3.3) can be treated as a set of equality constraints and can be appended to the original finite-element equation to form a modified matrix equation as

$$\begin{bmatrix} K & A^T \\ A & 0 \end{bmatrix} \begin{Bmatrix} \mathbf{x} \\ \lambda \end{Bmatrix} = \begin{Bmatrix} \mathbf{f} \\ \mathbf{c} \end{Bmatrix} \tag{3.6}$$

Reproduced with permission of the copyright owner. Further reproduction prohibited without permission.

where λ is the vector of Lagrange multipliers, A is made up of the coefficients of Eq.(3.3), and K and $\mathbf{f}$ are associated with the finite-element equation of the structure without an MPC:

$$K\mathbf{x}_0 = \mathbf{f} \tag{3.7}$$

where the solution $\mathbf{x}_0$ is different from $\mathbf{x}$ in Eq.(3.6).

With the above definitions, the efficient reanalysis technique discussed in chapter 2 can be used to find the exact solutions of the modified structures that result from the addition and removal of an MPC. An SPC is a special case of an MPC in which A is made up of unit vectors. That is, the only component in a row of A corresponds to the degree of freedom associated with the particular SPC. A typical example of an SPC is a roller support for a structure.

3.2 Addition of Linear Constraints

The Lagrange multipliers λ in Eq.(3.6), which are interface reactions, are considered to be unknowns in the following computational procedure. The compatibility of the displacements at the degrees of freedom at which the MPC is imposed and the internal equilibrium conditions between the interface reactions constitute a set of linear equations that can be solved for the interface reactions. The displacements at any point of the structure imposed with an MPC can then be calculated as a linear function of the interface reactions.

If the structure to be imposed with an MPC is linear and nonsingular, then the displacement $\mathbf{x}$ of the structure with the addition of the MPC is the solution of

$$K\mathbf{x} = \mathbf{f} - A^T\lambda \tag{3.8}$$

which is the upper part of Eq.(3.6). Subsequently, one obtains

$$\mathbf{x} = K^{-1}\mathbf{f} - K^{-1}A^T\lambda \tag{3.9}$$

Reproduced with permission of the copyright owner. Further reproduction prohibited without permission.

or

$$\mathbf{x} = \mathbf{x_0} + U\lambda \tag{3.10}$$

with Eq. (3.7),

$$K\mathbf{x_0} = \mathbf{f} \tag{3.11}$$

and

$$KU = -A^T \tag{3.12}$$

The lower part of Eq.(3.6) is associated with the MPC, which yields

$$A\mathbf{x} = \mathbf{c} \tag{3.13}$$

By substituting Eq.(3.10) for $\mathbf{x}$ in Eq.(3.13), one obtains a set of equations that can be solved for λ as

$$AU\lambda = \mathbf{c} - A\mathbf{x_0} \tag{3.14}$$

where AU is a $p \times p$ symmetric matrix. After the interface reactions have been determined, the displacements in every part of the structure can be calculated by using Eq.(3.10).

With the proposed procedure, Eq.(3.6) is not formed and solved for the displacement of the modified structure with MPC's. Instead, a set of equations is solved in the form of Eqs.(3.11) and (3.12). The number of new set of equations (Eq.(3.14)) is proportional to the number of MPC's; the dimension of these equations is much smaller than the dimension of the original equation (Eq.(3.6)).

For example, to find the solution of the modified structure in which nodes N_a and N_b are spot-welded together, one can solve two sets of six additional equations:

$$K\mathbf{x_{i,a}} = \mathbf{u_{i,a}}\,, \qquad \mathrm{i} = 1 \text{ through } 6 \tag{3.15}$$

Reproduced with permission of the copyright owner. Further reproduction prohibited without permission.

and

$$K\mathbf{x}_{i,b} = \mathbf{u}_{i,b}\,, \qquad i = 1 \text{ through } 6 \tag{3.16}$$

where pseudo force $\mathbf{u}_i$ is a unit force applied to one of 6 degrees of freedom associated with node N_a or N_b. The solution of the original structure without an MPC, subjected to the existing load $\mathbf{f}$, is given as

$$K\mathbf{x}_0 = \mathbf{f} \tag{3.17}$$

As a result, the displacement at node N_a can be obtained as

$$\mathbf{x}_a = \mathbf{x}_{i,a}\lambda_a + \mathbf{x}_{0a} \tag{3.18}$$

The same is true for $\mathbf{x}_b$. In Eq.(3.18), $\mathbf{x}_{i,a}$ is a subset of $\mathbf{x}_i$ that relates to node N_a only. The compatibility equation of Eq.(3.3) yields

$$\mathbf{x}_{i,a}\lambda_a + \mathbf{x}_{0a} = \mathbf{x}_{i,b}\lambda_b + \mathbf{x}_{0b} \tag{3.19}$$

and the equilibrium condition at the spot weld yields

$$\lambda_a = -\lambda_b \tag{3.20}$$

The combination of Eqs.(3.19) and (3.20) provides a set of 12 equations to solve λ. Once λ is found, the displacement of the modified structure can be obtained with the following equation:

$$\mathbf{x} = \mathbf{x}_i\lambda + \mathbf{x}_0 \tag{3.21}$$

Note that Eqs.(3.15) and (3.16) can be solved much faster than Eq.(3.6) for the modified displacement because the K matrix has already been factorized and only backward substitution is required to solve Eqs.(3.15) and (3.16). Furthermore, the bulk data file, the case control cards, and the force cards in the original MSC/NASTRAN file for solving Eq.(3.17) can be easily modified to solve Eqs.(3.15) and (3.16). The

Reproduced with permission of the copyright owner. Further reproduction prohibited without permission.

results can then be processed with an interface program to generate the solution of the modified structure. Thus, any commercially rated finite-element code can be incorporated into the reanalysis program discussed above to solve complicated, large-scale problems.

3.3 Removal of Linear Constraints

The modified Sherman-Morrison identity developed in chapter 2 is used here to analyze the modified structure with the removal of a linear constraint, without reforming and resolving Eq.(3.6).

Here, the finite-element equation for a structure without a linear constraint (Eq.(3.7)) is extended to the same dimension as that of Eq.(3.6); that is,

$$\begin{bmatrix} K & 0 \\ 0 & I \end{bmatrix} \begin{Bmatrix} \mathbf{x_0} \\ 0 \end{Bmatrix} = \begin{Bmatrix} \mathbf{f} \\ 0 \end{Bmatrix} \tag{3.22}$$

where I is an identity matrix whose dimension is equal to the number of linear constraints. By comparing Eq.(3.22) with Eq.(3.6), one can easily identify the left-hand-side matrix in Eq.(3.22)

$$\begin{bmatrix} K & 0 \\ 0 & I \end{bmatrix} \tag{3.23}$$

as the coefficient matrix K of Eq.(3.22), which is symmetric. The matrix modification, because of the presence of a linear constraint (Eq.(3.6)), is

$$\Delta K = -\begin{bmatrix} 0 & A^T \\ A & -I \end{bmatrix} \tag{3.24}$$

Thus,

$$\begin{bmatrix} K & 0 \\ 0 & I \end{bmatrix} = \begin{bmatrix} K & A^T \\ A & 0 \end{bmatrix} - \begin{bmatrix} 0 & A^T \\ A & -I \end{bmatrix} \tag{3.25}$$

The matrix modification ΔK can be defined and factorized as

$$\Delta K = -\sum \left(\nu_i E_i E_i^T \right) \tag{3.26}$$

Reproduced with permission of the copyright owner. Further reproduction prohibited without permission.

where ν_i and E_i are the eigenvalues and eigenvectors, respectively, of the modification matrix. As a result, Eq.(3.24) can be written in a matrix form as

$$-\begin{bmatrix} 0 & A^T \\ A & -I \end{bmatrix} = -VDV^T \tag{3.27}$$

where V is an $n \times m$ matrix made up of E_i, and D is an $m \times m$ diagonal matrix made up of ν_i. In particular, Eq.(3.24) can be symbolically expressed as the following equation for a spot weld with 1 degree of freedom:

$$-\begin{bmatrix} 0 & 0 & 1 \\ 0 & 0 & -1 \\ 1 & -1 & -1 \end{bmatrix} = -\left(E_1 E_1^T - 2E_2 E_2^T\right) \tag{3.28}$$

where eigenvectors E_1 and E_2 are $\left(\frac{1}{\sqrt{3}}, -\frac{1}{\sqrt{3}}, \frac{1}{\sqrt{3}}\right)^T$ and $\left(\frac{1}{\sqrt{6}}, -\frac{1}{\sqrt{6}}, -\frac{2}{\sqrt{6}}\right)^T$, respectively. The matrices V and D in Eq.(3.27) are then defined as

$$V = \begin{bmatrix} \frac{1}{\sqrt{3}} & \frac{1}{\sqrt{6}} \\ -\frac{1}{\sqrt{3}} & -\frac{1}{\sqrt{6}} \\ \frac{1}{\sqrt{3}} & -\frac{2}{\sqrt{6}} \end{bmatrix} \tag{3.29}$$

and

$$D = \begin{bmatrix} 1 & 0 \\ 0 & -2 \end{bmatrix} \tag{3.30}$$

Each spot weld has six pairs of nonzero eigenvalues and eigenvectors, such as those presented in Eq.(3.28).

After V and D have been identified, Eq.(2.3) can be recursively used to find the solution of the modified structure based on the solution of the original structure, without involving the new matrix inversion.

The procedure described in this section can also be applied to reanalyze a structure with the addition of linear constraints. However, in this case the modified coefficient matrix is related to the original one in the following manner:

$$\begin{bmatrix} K & A^T \\ A & 0 \end{bmatrix} = \begin{bmatrix} K & 0 \\ 0 & I \end{bmatrix} + \begin{bmatrix} 0 & A^T \\ A & -I \end{bmatrix} \tag{3.31}$$

Reproduced with permission of the copyright owner. Further reproduction prohibited without permission.

with

$$\Delta K = \begin{bmatrix} 0 & A^T \\ A & -I \end{bmatrix} = VDV^T \tag{3.32}$$

The major effort here to use the modified Sherman-Morrison identity for reanalyzing the modified structure is to solve

$$KQ = V \tag{3.33}$$

On the other hand, the major effort in the reanalysis procedure presented in section 3.2 is to solve

$$KU = -A^T \tag{3.34}$$

Therefore, if the dimension of A^T is less than V, as with SPC and MPC, then the method introduced in section 3.2 is a better choice than the method introduced here for reanalyzing a structure with the addition of linear constraints.

3.4 Computational Efficiency of Reanalysis Procedure

In order to study computational efficiency, a helpful procedure is to count the numerical operations involved in the proposed procedure. In accordance with the work of Kavlie and Powell [13], an operation is defined as a multiplication step plus an addition step, and only the major sequences of operations are counted. Let n be the dimension of the structure without spot welds, with b as the averaged bandwidth of its stiffness matrix, and let m be the total number of degrees of freedom at spot welds (each spot weld has 6 degrees of freedom). Thus, the dimension of A in Eq.(3.2) is $m \times n$.

3.4.1 Addition of Spot Welds

The major computation in analyzing a structure with a new set of spot welds includes solving U in Eq.(3.12) and solving a set of m equations associated with

Reproduced with permission of the copyright owner. Further reproduction prohibited without permission.

Eq.(3.14). The former requires the following number of operations:

$$N = \frac{nb^2}{2} + 3nmb - \left(\frac{3}{2}\right)mb^2 \tag{3.35}$$

The latter requires

$$N = \frac{m^3}{2} \tag{3.36}$$

operations, where the first term in Eq.(3.35) is for one matrix decomposition and the remainder of terms are for load-vector modifications and backward substitutions.

In the proposed optimization procedure for the pattern design of spot welds, U is only solved once, whereas equations in the form of Eqs.(3.12) and (3.14) are called frequently to analyze the structure with a new pattern of spot welds. Furthermore, U can be solved in advance. Thus, the total number of operations in the proposed optimization procedure is essentially

$$N = \frac{pm^3}{2} \tag{3.37}$$

where p is the number of new patterns that are reanalyzed in the design optimization process. For a problem with a large number of spot welds, Eq.(3.37) still represents an expensive computation; however, this computation is less costly than the standard analysis procedure, which involves the following number of operations:

$$N = \frac{npb^2}{2} + 3pnmb - \left(\frac{3}{2}\right)pmb^2 \tag{3.38}$$

and does not include the reformulation of the stiffness matrix.

3.4.2 Removal of Spot Welds

The major computation in the proposed procedure for removal of a spot weld involves the solution of the following equation:

$$KQ = V \tag{3.39}$$

Reproduced with permission of the copyright owner. Further reproduction prohibited without permission.

where Q represents the 12 eigenvectors associated with 1 spot weld, as indicated by Eq.(3.24); K in Eq.(3.39) does not need to be factorized because Eq.(3.39) is in the same form as Eq.(3.7). The number of operations is essentially

$$\mathrm{N} = 36n\mathrm{b} - 18\mathrm{b}^2 \tag{3.40}$$

which, obviously, is more efficient than a standard analysis.

3.5 Application to SPC

An SPC is a special case of an MPC. In particular, each row of matrix A has only a nonzero component, which simplifies the computation. Equations (3.11), (3.12), and (3.14) are still valid for the addition of an SPC, as is Eq.(2.9) for the removal of an SPC. Nevertheless, the ΔK for an SPC is symbolically given as

$$-\begin{bmatrix} 0 & 1 \\ 1 & -1 \end{bmatrix} \tag{3.41}$$

whose associated eigenvalues ν_1 and ν_2 are $\frac{-1+\sqrt{5}}{2}$ and $\frac{-1-\sqrt{5}}{2}$, respectively, and the normalized eigenvectors E_1 and E_2 are $(-0.8506, -0.5257)^{\mathrm{T}}$ and $(0.5257, -0.8506)^{\mathrm{T}}$, respectively. Therefore, the matrices V and D in Eq.(3.27) should be modified as

$$V = \begin{bmatrix} -0.8506 & 0.5257 \\ -0.5257 & -0.8506 \end{bmatrix} \tag{3.42}$$

and

$$D = \begin{bmatrix} \frac{-1+\sqrt{5}}{2} & 0 \\ 0 & \frac{-1-\sqrt{5}}{2} \end{bmatrix} \tag{3.43}$$

Reproduced with permission of the copyright owner. Further reproduction prohibited without permission.

CHAPTER 4

ANALYTICAL EXAMPLES

A cantilever beam is used as an example to demonstrate the reanalysis procedure for a structure for which the support conditions are being modified. The beam is discretized into two elements, each 100 in. in length. A vertical and a horizontal force of –700 and 500 lb, respectively, is applied at node 2, as shown in Fig. 4.1. The sectional properties of the beam, EI and EA are 15E+6 lb-in^2 and 45E+6 lb,

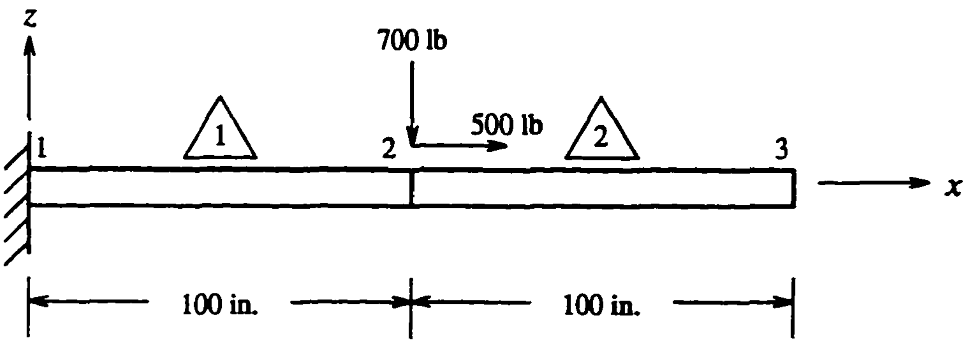

Figure 4.1. Cantilever beam.

respectively. This study uses the standard beam finite element, which has 3 degrees of freedom at a node: the axial displacement u, the lateral displacement w, and the rotation θ. The finite-element equation of the beam is given as

$$K\mathbf{x}_0 = \mathbf{f}_0 \tag{4.1}$$

where the reduced-order stiffness matrix K for the beam is obtained as

$$K = 10^4 * \begin{bmatrix} 90 & 0 & 0 & -45 & 0 & 0 \\ 0 & 0.036 & 0 & 0 & -0.018 & 0.9 \\ 0 & 0 & 120 & 0 & -0.9 & 30 \\ -45 & 0 & 0 & 45 & 0 & 0 \\ 0 & -0.018 & -0.9 & 0 & 0.018 & -0.9 \\ 0 & 0.9 & 30 & 0 & -0.9 & 60 \end{bmatrix} \tag{4.2}$$

Reproduced with permission of the copyright owner. Further reproduction prohibited without permission.

the force $\mathbf{f}_0$ is equal to $(500, -700, 0, 0, 0, 0)^T$ lb, and the solution of the problem $\mathbf{x}_0$ is $(0.00111, -15.55556, -0.23333, 0.00111, -38.88889, -0.23333)^T$ in.

4.1 Addition of Simple Support

This example analyzes the beam shown in Fig. 4.1, with a support added to node 3. The modified beam is shown in Fig. 4.2.

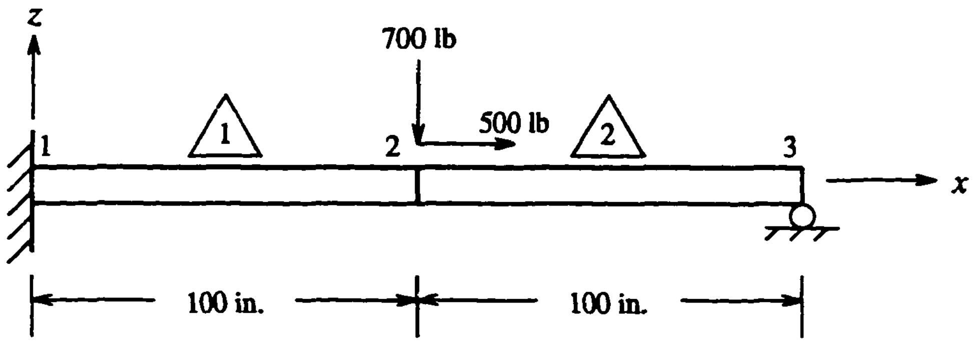

Figure 4.2. Beam with simple support at node 3.

The solution of the modified beam can be obtained, with the help of a Lagrange multiplier, by the equation

$$\overline{K}\mathbf{x} = \mathbf{f} \tag{4.3}$$

where the augmented stiffness matrix $\overline{K}$ is given as

$$\overline{K} = 10^4 \cdot \begin{bmatrix} 90 & 0 & 0 & -45 & 0 & 0 & 0 \\ 0 & 0.036 & 0 & 0 & -0.018 & 0.9 & 0 \\ 0 & 0 & 120 & 0 & -0.9 & 30 & 0 \\ -45 & 0 & 0 & 45 & 0 & 0 & 0 \\ 0 & -0.018 & -0.9 & 0 & 0.018 & -0.9 & 10^{-4} \\ 0 & 0.9 & 30 & 0 & -0.9 & 60 & 0 \\ 0 & 0 & 0 & 0 & 10^{-4} & 0 & 0 \end{bmatrix} \tag{4.4}$$

the force $\mathbf{f}$ is $(500, -700, 0, 0, 0, 0, 0)^T$, and the solution $\mathbf{x}$ is $(u_2, w_2, \theta_2, u_3, w_3, \theta_3, \lambda)^T$ in which λ is equal to the reaction R at the additional support with an opposite sign. The exact value of $\mathbf{x}$ is obtained from Eq.(4.3) as $(0.00111, -3.40278, -0.01458, 0.00111, 0, 0.05833, -218.75)^T$ in.

Reproduced with permission of the copyright owner. Further reproduction prohibited without permission.

However, one can find the solution of the modified beam by using the original stiffness matrix given by Eq.(4.2) based on the procedure discussed in section 3.2. In this process, one applies a single unit of force along the z axis to node 3 to obtain the displacement $\mathbf{x_1} = (0, 0.05556, 0.00100, 0, 0.17778, 0.00133)^T$. One then obtains the reaction force R at node 3 of the modified beam, based on the condition that the vertical displacement at node 3 should maintain zero. That is,

$$0.17778R - 38.88889 = 0 \tag{4.5}$$

which yields a reaction of 218.75. The exact solution $\mathbf{x}$ for the modified beam can be obtained with the relation

$$\mathbf{x} = \mathbf{x_1} * R + \mathbf{x_0} \tag{4.6}$$

Note that in the process discussed above, $\overline{K}$ of Eq.(4.4) does not need to be formed and Eq.(4.3) does not need to be solved.

4.2 Removal of Simple Support

Here, the support at node 3 is now removed from the structure shown in Fig. 4.2. In this case, $\overline{K}$ of Eq.(4.4) has been formed, and $\mathbf{x}$ has been found by solving Eq.(4.3). The task here is to find the solution $\mathbf{x_0}$ of the beam with the simple support removed by taking the advantage of the fact that $\mathbf{x}$ is known and that $\overline{K}$ has been factorized.

By comparing $\overline{K}$ of Eq.(4.4) with K of Eq.(4.2), ΔK can be conveniently identified for this problem as

$$\Delta K = \begin{bmatrix} 0 & 0 & 0 & 0 & 0 & 0 & 0 \\ 0 & 0 & 0 & 0 & 0 & 0 & 0 \\ 0 & 0 & 0 & 0 & 0 & 0 & 0 \\ 0 & 0 & 0 & 0 & 0 & 0 & 0 \\ 0 & 0 & 0 & 0 & 0 & 0 & 1 \\ 0 & 0 & 0 & 0 & 0 & 0 & 0 \\ 0 & 0 & 0 & 0 & 1 & 0 & -1 \end{bmatrix} \tag{4.7}$$

$$= \nu_1 E_1 E_1^T + \nu_2 E_2 E_2^T \tag{4.8}$$

Reproduced with permission of the copyright owner. Further reproduction prohibited without permission.

$$= \frac{-1+\sqrt{5}}{2} \cdot \begin{Bmatrix} 0 \\ 0 \\ 0 \\ 0 \\ -0.8506 \\ 0 \\ -0.5257 \end{Bmatrix} \cdot \begin{Bmatrix} 0 \\ 0 \\ 0 \\ 0 \\ -0.8506 \\ 0 \\ -0.5257 \end{Bmatrix}^T + \frac{-1-\sqrt{5}}{2} \cdot \begin{Bmatrix} 0 \\ 0 \\ 0 \\ 0 \\ 0.5257 \\ 0 \\ -0.8506 \end{Bmatrix} \cdot \begin{Bmatrix} 0 \\ 0 \\ 0 \\ 0 \\ 0.5257 \\ 0 \\ -0.8506 \end{Bmatrix}^T \tag{4.9}$$

The solution of the beam without the right-end support is given by applying Eq.(2.6) as

$$\mathbf{x}_0 = \mathbf{x} + \nu_1 Q_1 \left(E_1^T \mathbf{x}_0 \right) + \nu_2 Q_2 \left(E_2^T \mathbf{x}_0 \right) \tag{4.10}$$

The vectors Q_1 and Q_2 are obtained as $(0, -0.1643, -0.0030, 0, -0.5257, -0.0039, 2.1065)^T$ and $(0, -0.2658, -0.0048, 0, -0.8506, -0.0064, 5.3103)^T$ by solving $\overline{K}Q_1 = E_1$ and $\overline{K}Q_2 = E_2$. Note that Q_1 and Q_2 are also the solutions of the beam with the right-end support, subjected to loads, $(0, 0, 0, 0, -0.8506, 0)^T$ and $(0, 0, 0, 0, 0.5257, 0)^T$ and to the nonhomogeneous constraints that the z direction displacements at node 3 are prescribed as -0.5257 and -0.8506, respectively.

The values of $\left(E_1^T \mathbf{x}_0\right)$ and $\left(E_2^T \mathbf{x}_0\right)$ in Eq.(4.10) can be obtained by using the known vectors E_1, E_2, Q_1, Q_2, and $\mathbf{x}$ for the problem of concern to compute

$$\begin{aligned} E_1^T Q_1 &= -0.6602 \\ E_1^T Q_2 &= -2.0681 \\ E_2^T Q_1 &= -2.0681 \\ E_2^T Q_2 &= -4.9641 \\ E_1^T \mathbf{x} &= 114.9969 \\ E_2^T \mathbf{x} &= 186.0688 \end{aligned} \tag{4.11}$$

Reproduced with permission of the copyright owner. Further reproduction prohibited without permission.

which constitute the desired matrix equation

$$\begin{bmatrix} 1.4080 & -3.3462 \\ 1.2781 & -7.0320 \end{bmatrix} \begin{Bmatrix} E_1^T \mathbf{x_0} \\ E_2^T \mathbf{x_0} \end{Bmatrix} = \begin{Bmatrix} 114.9969 \\ 186.0688 \end{Bmatrix} \tag{4.12}$$

This matrix equation, in turn, gives the values of $(E_1^T \mathbf{x_0})$ and $(E_2^T \mathbf{x_0})$ as 33.0757 and -20.4488, respectively. Finally, the solution of the modified beam can be calculated by using Eq.(4.10) as $\mathbf{x_0}$ = (0.00111, -15.55556, -0.23333, 0.00111, -38.88889, -0.23333)^T.

Note that the exact solution of the modified beam has been recovered without forming the corresponding stiffness matrix K.

4.3 Addition of Inclined Support

This example analyzes a modified beam, shown in Fig. 4.3, which is obtained by adding an inclined support to node 3 of the original beam (Fig. 4.1). The inclined support yields an MPC as

$$u_3 \sin\theta - w_3 \cos\theta = 0 \tag{4.13}$$

where u_3 and w_3 are the axial and vertical displacements at node 3, respectively.

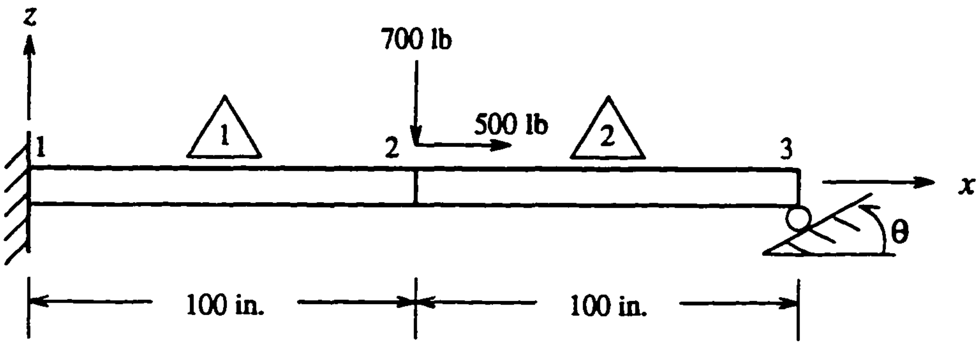

Figure 4.3. Beam with inclined support at node 3.

Similar to the example in section 4.1, the solution of the modified beam can be obtained by the equation

$$\overline{K}\mathbf{x} = \mathbf{f} \tag{4.14}$$

Reproduced with permission of the copyright owner. Further reproduction prohibited without permission.

where the augmented stiffness matrix is given as

$$\overline{K} = 10^4 * \begin{bmatrix} 90 & 0 & 0 & -45 & 0 & 0 & 0 \\ 0 & 0.036 & 0 & 0 & -0.018 & 0.9 & 0 \\ 0 & 0 & 120 & 0 & -0.9 & 30 & 0 \\ -45 & 0 & 0 & 45 & 0 & 0 & \sin\theta/10^4 \\ 0 & -0.018 & -0.9 & 0 & 0.018 & -0.9 & -\cos\theta/10^4 \\ 0 & 0.9 & 30 & 0 & -0.9 & 60 & 0 \\ 0 & 0 & 0 & \sin\theta/10^4 & -\cos\theta/10^4 & 0 & 0 \end{bmatrix} \quad (4.15)$$

The force f in Eq.(4.14) is (500, –700, 0, 0, 0, 0, 0)^T, and the solution x is $(u_2, w_2, \theta_2, u_3, w_3, \theta_3, \lambda)^T$, in which the Lagrange multiplier λ is equal to the reaction R at the additional support with an opposite sign. If θ is equal to 30°, then the exact value of x is obtained from Eq.(4.14) as (0.00083, –3.4027, –0.01458, 0.00055, 0.00032, 0.05834, 252.60)^T.

The solution of the modified beam can be found by using the original matrix equation of Eq.(4.2), based on the procedure discussed in section 3.2. In this process, one applies a single unit of force along the direction of R at node 3, which is equal to $(0, 0, 0, -\sin\theta, \cos\theta, 0)$, with which the solution of Eq.(3.12) results in U = (–0.000001, 0.04811, 0.00087, –0.000002, 0.15396, 0.00115)^T for θ = 30°. The constraint condition of Eq.(4.13) can be used to find the reaction force R at node 3 of the modified beam as

$$\left(u_3^{'}R + u_3\right)\sin\theta - \left(w_3^{'}R + w_3\right)\cos\theta = 0 \quad (4.16)$$

where $\left(u_3^{'}R + u_3\right)$ and $\left(w_3^{'}R + w_3\right)$ are the total displacements at node 3. More specifically, $u_3^{'} = -0.000002$, $w_3^{'} = 0.15396$, $u_3 = 0.00111$, and $w_3 = -38.88889$, where u_3 and w_3 are the displacements at node 3 of the structure shown in Fig. 4.1. With known values of $u_3^{'}$, u_3, $w_3^{'}$, w_3, and θ, Eq.(4.16) gives a reaction of 252.6. Note that Eq.(4.16) is in the same form as Eq.(3.14). Finally, the exact solution x for the modified beam can then be obtained with the relation of Eq.(3.10) as

$$\mathbf{x} = \mathbf{x}_0 + UR \quad (4.17)$$

Reproduced with permission of the copyright owner. Further reproduction prohibited without permission.

4.4 Removal of Inclined Support

The procedure demonstrated here is for the removal of the inclined support at node 3 of the structure shown in Fig. 4.3. In this case, $\overline{K}$ in Eq.(4.15) has been formed, and x has been determined by solving Eq.(4.14). The task here is to take the advantage of the fact that x is known and $\overline{K}$ has been factorized to find the solution x_0.

By comparing $\overline{K}$ in Eq.(4.15) and K in Eq.(4.2), ΔK may be conveniently identified for this problem as

$$\Delta K = \begin{bmatrix} 0 & 0 & 0 & 0 & 0 & 0 & 0 \\ 0 & 0 & 0 & 0 & 0 & 0 & 0 \\ 0 & 0 & 0 & 0 & 0 & 0 & 0 \\ 0 & 0 & 0 & 0 & 0 & 0 & \sin\theta \\ 0 & 0 & 0 & 0 & 0 & 0 & -\cos\theta \\ 0 & 0 & 0 & 0 & 0 & 0 & 0 \\ 0 & 0 & 0 & \sin\theta & -\cos\theta & 0 & -1 \end{bmatrix} \tag{4.18}$$

The ΔK can be decomposed as

$$\Delta K = \nu_1 E_1 E_1^T + \nu_2 E_2 E_2^T \tag{4.19}$$

where ν_i and E_i are the ith eigenpair of ΔK. That is,

$$\Delta K = \frac{-1+\sqrt{5}}{2} \bullet \begin{Bmatrix} 0 \\ 0 \\ 0 \\ 0.618\sin\theta/r \\ -0.618\cos\theta/r \\ 0 \\ 0.3819/r \end{Bmatrix} \bullet \begin{Bmatrix} 0 \\ 0 \\ 0 \\ 0.618\sin\theta/r \\ -0.618\cos\theta/r \\ 0 \\ 0.3819/r \end{Bmatrix}^T + \frac{-1-\sqrt{5}}{2} \bullet \begin{Bmatrix} 0 \\ 0 \\ 0 \\ -1.618\sin\theta/s \\ 1.618\cos\theta/s \\ 0 \\ 2.6179/s \end{Bmatrix} \bullet \begin{Bmatrix} 0 \\ 0 \\ 0 \\ -1.618\sin\theta/s \\ 1.618\cos\theta/s \\ 0 \\ 2.6179/s \end{Bmatrix}^T \tag{4.20}$$

where $r = \left\{0.618^2 \sin^2\theta + (-0.618)^2 \cos^2\theta + 0.3819^2\right\}^{1/2}$ and $s = \left\{(-1.618)^2 \sin^2\theta + 1.618^2 \cos^2\theta + 2.6179^2\right\}^{1/2}$.

The solution of the beam without the right-end support can be solved by Eq.(4.10). If θ is assumed to be 30°, $\sin\theta$ is 0.5 and $\cos\theta$ is 0.866. Then, the vectors Q_1 and Q_2

Reproduced with permission of the copyright owner. Further reproduction prohibited without permission.

are obtained as (0.000004, −0.1897, −0.0034, 0.000009, −0.6070, −0.0046, −3.0923)^T and (0.000007, −0.3069, −0.0055, 0.00001, −0.9822, −0.0074, −6.9056)^T by solving $\overline{K}Q_1 = E_1$ and $\overline{K}Q_2 = E_2$. Note that Q_1 and Q_2 are also the solutions of the beam with the right-end support, subjected to loads (0, 0, 0, 0.4253, −0.7367, 0)^T and (0, 0, 0, −0.2629, 0.4553, 0)^T and to the nonhomogeneous constraints that the R-direction displacements at node 3 are prescribed as 0.5257 and 0.8506, respectively.

The values of $\left(E_1^T \mathbf{x}_0\right)$ and $\left(E_2^T \mathbf{x}_0\right)$ can be obtained by using the known vectors E_1, E_2, Q_1, Q_2, and $\mathbf{x}$ to first compute

$$\begin{aligned} E_1^T Q_1 &= -1.1784 \\ E_1^T Q_2 &= -2.9067 \\ E_2^T Q_1 &= -2.9067 \\ E_2^T Q_2 &= -6.3211 \\ E_1^T \mathbf{x} &= 132.7919 \\ E_2^T \mathbf{x} &= 214.8617 \end{aligned} \tag{4.21}$$

and then constitute the desired matrix equation

$$\begin{bmatrix} 1.7282 & -4.7030 \\ 1.7963 & -9.2275 \end{bmatrix} \begin{Bmatrix} E_1^T \mathbf{x}_0 \\ E_2^T \mathbf{x}_0 \end{Bmatrix} = \begin{Bmatrix} 132.7919 \\ 214.8617 \end{Bmatrix} \tag{4.22}$$

which in turn gives the values of $\left(E_1^T \mathbf{x}_0\right)$ and $\left(E_2^T \mathbf{x}_0\right)$ as 28.6490 and −17.7078, respectively. Finally, the solution of the modified beam can be calculated by using Eq.(4.10) as $\mathbf{x}_0$ = (0.00111, −15.55556, −0.23333, 0.00111, −38.88889, −0.23333)^T. Again, note that the exact solution of the modified beam has been recovered without forming the corresponding stiffness matrix K.

Reproduced with permission of the copyright owner. Further reproduction prohibited without permission.

CHAPTER 5

APPLICATION OF REANALYSIS TECHNIQUES FOR OPTIMUM PLACEMENT OF SPOT WELDS

A design optimization scheme that provides a systematic procedure to determine the minimum number of spot welds required and the best locations to place these spot welds is introduced in this chapter. The key elements of this scheme are a genetic algorithm and the reanalysis technique presented in chapters 3 and 4.

5.1 Introduction

Spot welding is a basic type of solid resistance welding [19]. Squeeze time, weld time, hold time, and off time are the fundamental variables in spot welding. For welding most metals, but especially the nonferrous types, these variables must be controlled within very close limits.

Spot welds are made by first cleaning the two pieces of metal to be lapped and placing them between the copper electrodes of the spot-welding machine. During the squeeze time, the two pieces of metal are brought together. A current flows through the electrodes during the weld time, which causes a nugget to form at the interface of the two pieces of metal. The hold time is basically a cooling period; this period is the interval from the end of the current flow until the electrodes part. The water-cooled electrodes transfer the heat rapidly away from the weld. The off time is the interval during which the electrodes are apart before the cycle automatically repeats for the next weld. If this portion of the control is switched off, then the machine will stop after each weld.

Reproduced with permission of the copyright owner. Further reproduction prohibited without permission.

The weld that is produced by the sequence described above contains three distinctive features, as shown in Fig. 5.1 [20]. The central region where the metal has been melted has a cast structure that is typical of fusion welds, with columnar grains that meet at the line of the original interface. Surrounding the weld nugget is a heat-affected zone, which shows that the parent metal has undergone a heating and cooling cycle. The outer surfaces of the sheets show indentations that result from the pressure of the electrode tips. The reduction in thickness of the sheet at this point should not be more than 10 percent under normal conditions.

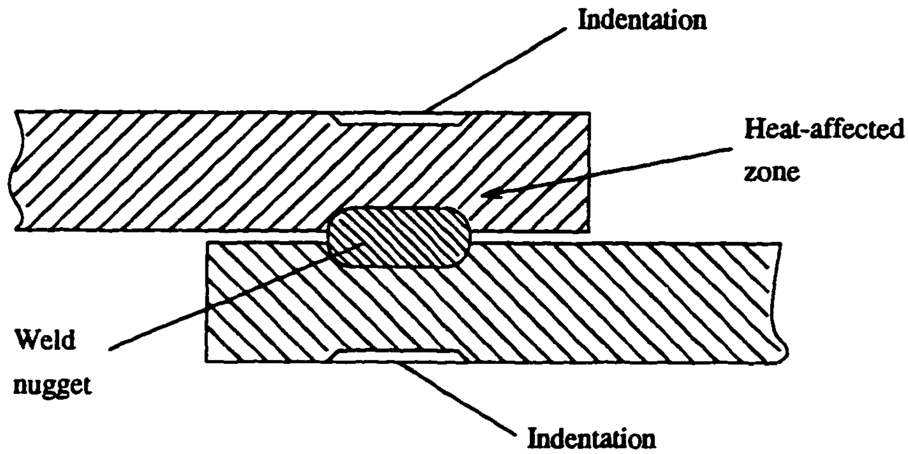

Figure 5.1. Features of spot weld.

A direct relationship exists between the weld strength of a given joint and its design. The factors that must be taken into consideration for a given material are the amount of overlap, the spot spacing, and the weld size. An acceptable weld size for a thickness range of 0.032 to 0.188 in. (0.08128 cm to 0.47752 cm) is roughly 0.10 in. (0.254 cm) plus two times the thickness of the thinnest member. The overlap should be equal to two times the weld size plus 0.125 in. (0.3175 cm). (The 0.125 in. value is the tolerance for positioning the weld.) If fixturing is used to center the spot in the overlap, then the 0.125 in. (0.3175 cm) tolerance can be disregarded.

Welds placed too close to the edge will often squirt to the previous weld and, thus, reduce the size of the weld that is made. A general rule is to allow 16t between welds,

Reproduced with permission of the copyright owner. Further reproduction prohibited without permission.

where t is the thickness of the material. However, if the elimination of distortion is more important than strength, this figure should be increased to $48t$.

5.2 Optimum Placement of Spot Welds

The design-optimization problem for spot-weld placement is to select the minimum number of spot welds from a predetermined set, subject to the constraint that the modified structure should perform satisfactorily in terms of structural strength and rigidity.

To begin this placement design scheme, one can specify N number of possible locations to place spot welds. This set of design candidates for the spot welds constitutes the design space. Two design choices exist for each of the candidate positions in the design space: the space is either selected for spot welding or it is not selected. Therefore, the potential number of arrangements for placing the spot welds is 2^N. This problem is a typical design-optimization problem with discrete design variables. Here, a genetic algorithm is applied for this type of application. The major steps of the proposed approach are depicted in Fig. 5.2. The reanalysis technique in conjunction with a genetic-algorithm code is used to find the best placement for the spot welds. The reanalysis technique indicated in Fig. 5.2 (introduced in chapters 3 and 4) is used to reanalyze the performance of the modified structure with the new spot-weld pattern.

Thus, in the optimization procedure, equations similar to Eq.(3.15) must be solved for each spot-weld pattern. Subsequently, the performance of each of the design alternatives can be evaluated and used by the design-optimization algorithm to generate an improved design.

Reproduced with permission of the copyright owner. Further reproduction prohibited without permission.

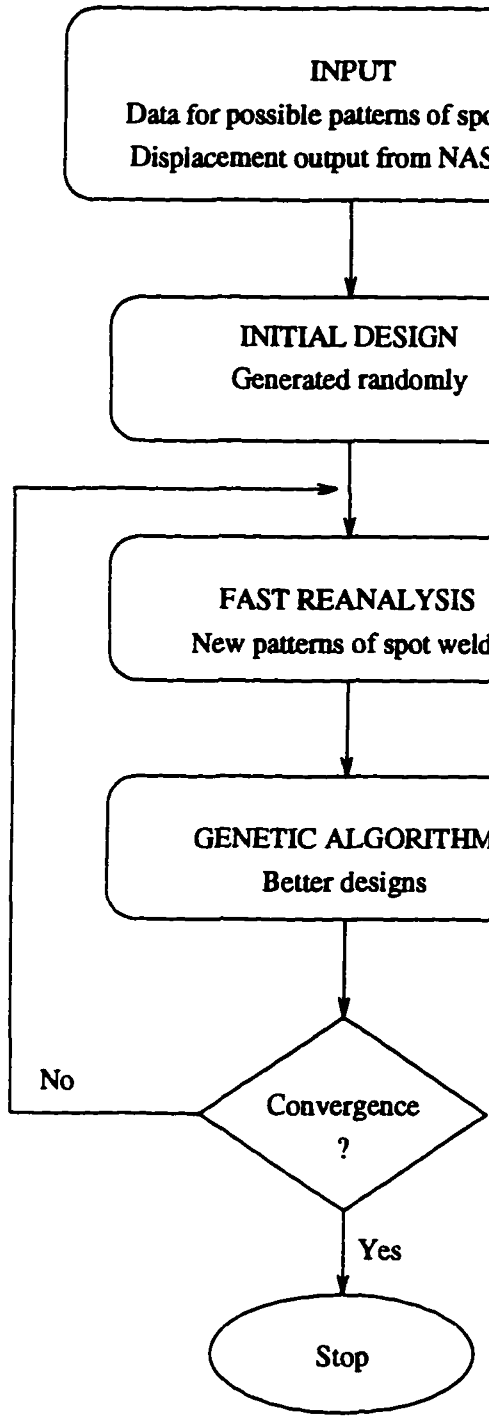

Figure 5.2. Solution process for optimal pattern design of spot welds.

Reproduced with permission of the copyright owner. Further reproduction prohibited without permission.

5.3 Genetic Algorithm

A genetic algorithm is a numerical procedure that produces a set of better designs; the principle behind this algorithm is the process of natural evolution [17] (i.e., Darwin's theory of the survival of the fittest). Evolution primarily relies on the random generation of new designs, from which only the superior designs survive to participate in future reproduction. Initially, a set of designs, called the population of designs, is generated randomly. The designs are evaluated and ranked, based on certain criteria, before the reproduction process begins. The designs in this population are then selected, with favor given to the superior designs, to mate (called crossover) and produce a new set of designs. Some of these new designs are again selected to undergo other reproductive mechanisms, such as mutation and permutation, which are also commonly found in the process of evolution.

Genetic algorithms have been applied to many engineering design-optimization problems and have been proved to be effective for both nonconvex and nondifferentiable types of problems. The most attractive feature of such algorithms is that they have the ability to locate the global minimum, whereas gradient-based algorithms often converge to a local minimum. Because genetic algorithms work according to Darwin's theory, the good chromosomes, called schema, which are attributed to the good characteristics of the design, will be preserved and accumulated throughout the reproduction process to eventually lead to the best global design.

A string of integers is usually used in a genetic algorithm to symbolically represent an individual design. The integers play the role of the chromosomes in biology. The determination of the correspondence between the integers and the numerical values of the physical design variables is called the coding process. For example, a design alternative for a 10-bar truss can be represented by a string of 10 integers. If each of the integers ranges from 1 to 4, then each truss member has up to four possibilities

Reproduced with permission of the copyright owner. Further reproduction prohibited without permission.

in its properties and size.

The reproduction process is performed by manipulating the chromosomes (i.e., the integers in a genetic algorithm) of the parent designs. Three major operations shown in Fig. 5.3 are implemented in this study for this manipulation: crossover, mutation, and permutation. The determination of whether any of these operations will be activated to modify the designs is, again, a random process.

Crossover is simply a mating process in biological terms. In this operation, chromosomes from a pair of parent designs are exchanged to produce child designs. The crossover points are determined randomly. Mutation, on the other hand, is modeled after the sudden change that can occur in chromosomes in biology. Any integer in a design string can be selected to undergo this random change. Finally, permutation simply reverses the order of chromosomes in a design string.

Next, a genetic algorithm evaluates, ranks, and selects some of the child designs for creation of the next generation. The life cycle continues until no improvement is realized within a certain predetermined number of consecutive generations. A computational flowchart for a basic genetic algorithm is shown in Fig. 5.4.

Although genetic algorithms are simple to implement, the quality of the results depends primarily on certain input parameters, such as the size of the population and the parameters that control the occurrence of certain reproduction processes. A smaller population may not produce better designs. On the other hand, a larger population may require a larger number of function evaluations; hence, more computational time is required. In general, a population size equal to three times the length of the integer string is recommended. In addition, during the reproduction process, a high probability should be assigned to the crossover and permutation processes, and a low probability should be assigned to the mutation process.

A genetic algorithm ranks the performance of each design by evaluating a

Reproduced with permission of the copyright owner. Further reproduction prohibited without permission.

single-valued function. Hence, the genetic algorithm can be directly applied to an unconstrained minimization problem. To solve the constrained minimization problem, the problem must be converted into an equivalent unconstrained minimization problem by using the penalty function method [16]. For example, a typical constrained minimization problem can be stated as

$$\min_{b} \qquad F(b) \tag{5.1}$$

subject to

$$\begin{aligned} g_i(b) &< 0, & i &= 1,2,...,p \\ h_j(b) &= 0, & j &= 1,2,...,q \end{aligned} \tag{5.2}$$

where F is the objective function, b are the design variables, and g and h are the inequality and equality constraints, respectively. This constrained minimization problem can be converted to an equivalent unconstrained minimization problem by using a penalty function. For example, by using an exterior penalty function, the problem can be written as

$$\min_{b} \qquad \Psi(b) = F(b) + r' \sum_{i=1}^{p} (g_i + |g_i|)^2 + s' \sum_{j=1}^{q} (h_j)^2 \tag{5.3}$$

where r' and s' are the penalty coefficients that are used to penalize those designs that violate the constraints. Now the single-valued merit function Ψ can be directly used to rank various designs in the population.

Reproduced with permission of the copyright owner. Further reproduction prohibited without permission.

CROSSOVER

Parent 1	Parent 2
3 1 4 / 2 2 3 1 4	1 4 2 / 4 3 1 4 1

Crossover location

Child 1	Child 2
3 1 4 / 4 3 1 4 1	1 4 2 / 2 2 3 1 4

(a) Crossover operation between two parent chromosomes.

MUTATION

Before mutation $\longrightarrow$ 1 4 2 2 2 3 1 4

Mutation location

After mutation $\longrightarrow$ 1 4 2 3 2 3 1 4

(b) Mutation operation in string.

PERMUTATION

Before permutation $\longrightarrow$ 1 4 4 3 2 3 1 4

Permutation location

After permutation $\longrightarrow$ 1 4 2 3 4 3 1 4

(c) Permutation operation in string.

Figure 5.3. Three major operations in genetic algorithm.

Reproduced with permission of the copyright owner. Further reproduction prohibited without permission.

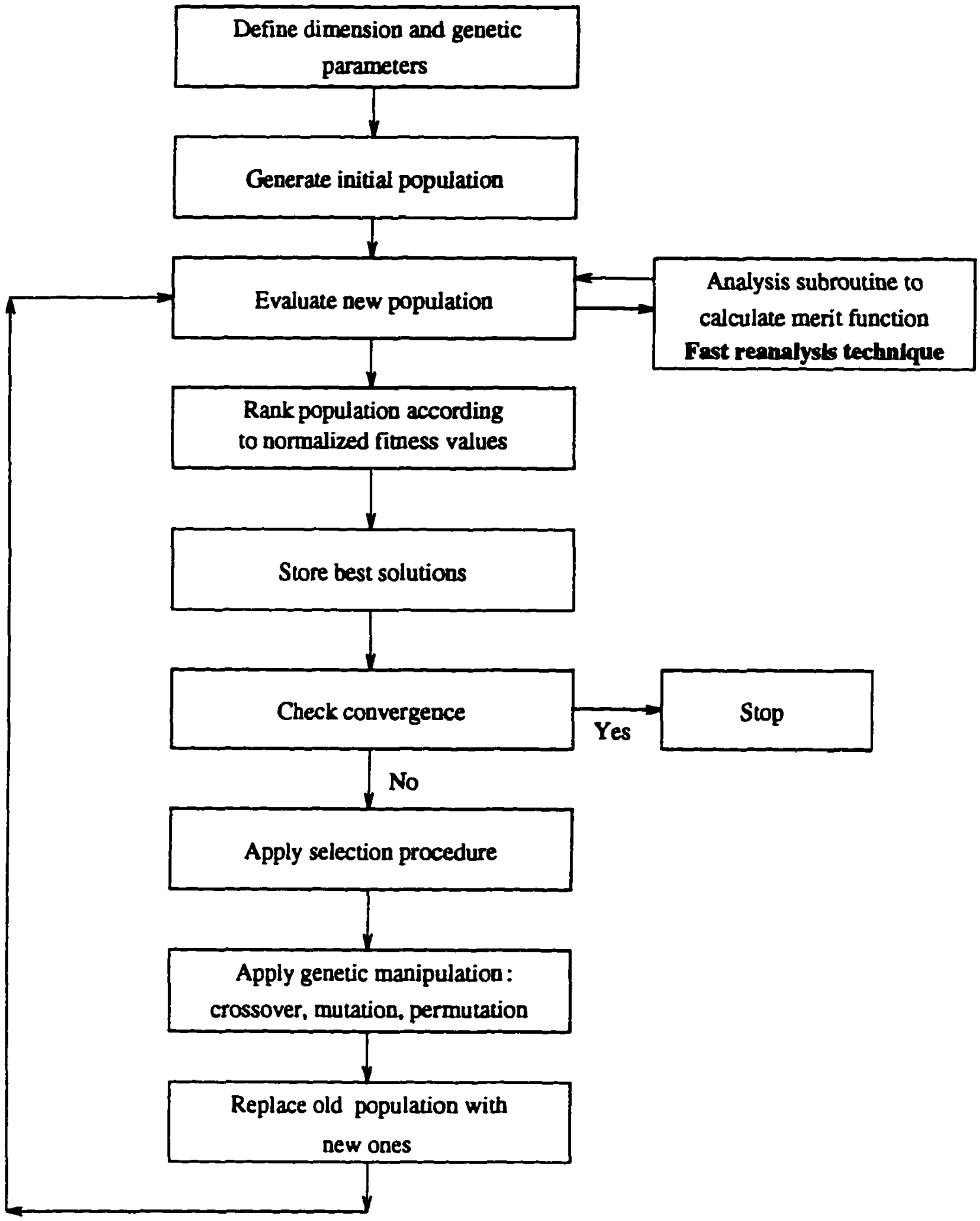

Figure 5.4. Basic flowchart associated with genetic algorithm.

Reproduced with permission of the copyright owner. Further reproduction prohibited without permission.

5.4 Numerical Implementation

The proposed computational procedure has a major advantage in reanalysis in that it does not involve any modification of the stiffness matrix; thus, this procedure can be conveniently interfaced with any commercially rated finite-element analysis codes. In our initial numerical experiments, MSC/NASTRAN is used to find Q in Eq. (2.10). Code modules are developed to solve Eqs.(3.9), (3.11), and (2.1), which are incorporated with the genetic algorithm.

The most difficult part of the proposed approach for optimum spot-weld pattern design is the mathematical formulation of the problem to properly measure the quality of a pattern of spot welds. This study focuses on three performance criteria: maximizing the rigidity of the welding structure, minimizing the number of spot welds, and maintaining a satisfactory stress level in spot welds. These criteria are blended into a single merit function with weighting coefficients assigned to each. The genetic algorithm then uses the merit functions of different designs as a guideline to perform genetic evolution and eventually produce better designs.

5.5 Application Examples

Two examples are presented here to evaluate the developed computational procedure. These sample problems also facilitate the study of design-problem formulation for optimum spot-weld pattern design. The structural components to be welded together in these two examples are all fully constrained.

The design variables in the examples are the patterns of spot welds. Each design variable is represented as a string of integers (with a value of 1 or 2). The length of the string is the same as the number of the candidate spots in which the welds are to be placed. Each integer in the string corresponds to a candidate spot. A 1 indicates that the candidate location has not been selected for a weld; a 2 indicates that the candidate location has been selected. If the number of possible locations for

Reproduced with permission of the copyright owner. Further reproduction prohibited without permission.

spot welds is m, then the developed computational procedure will select the best ones from among the 2^m possible patterns of spot welds.

Several criteria, including the number and the strength of the spot welds and the rigidity of the welded structure, are selected in this study to measure the performance of any pattern of spot welds. These criteria can be mathematically formulated as a constrained design-optimization problem as

$$\min \quad N \tag{5.4}$$

subjected to :

$$a_i < a_o, \qquad i = 1 \; to \; N \tag{5.5}$$

$$C < C_o \tag{5.6}$$

where N is the number of spot welds, a_i is a measurement of the state of stresses in spot weld i, and C represents the compliance of the structure.

In the problem formulation of Eqs.(5.4) to (5.6), the objective function is defined as the number of spot welds so as to minimize the manufacturing cost of spot welds. The stress constraint prevents spot welds from being overloaded, and the compliance constraint ensures the minimum rigidity of the welded structure. The compliance is calculated as the work done by the external forces. A higher compliance implies a lower rigidity of the welded structure. Equation (5.6) specifies the upper bound of the compliance as C_o, which is the compliance of the welded structure with all of its candidate spots filled with welds. Thus, the constraint of Eq.(5.6) is expected to be violated or at most to be a tight constraint because C_o has the least value among all possible spot-weld patterns.

The use of stress values is the most direct way to establish the constraint of Eq.(5.5). However, for simplicity, the internal forces at the spot welds, which are proportional to the stresses, are directly used to measure the strength of spot welds in this study. A more sophisticated method for calculating the strength of spot welds can be found in Ref. [18].

Reproduced with permission of the copyright owner. Further reproduction prohibited without permission.

Because the genetic algorithm can be applied to the unconstrained maximization problem only, the above-stated design optimization must be converted into an unconstrained problem. To this end, a composite function is generated to characterize the above-stated problem as a reciprocal of a product of three quantities:

$$F = 1/\{(N+1)(S+1)(W+1)\} \tag{5.7}$$

where the first term is associated with the number of the spot welds and the other terms are associated with the constraints defined by Eqs.(5.5) and (5.6). More specifically, S is defined as

$$S = \sum_{i=1}^{n} \{(a_i - a_o) + |(a_i - a_o)|\} \tag{5.8}$$

which yields a positive value if the reaction force on any of the spot welds is greater than the desired bound. In addition, W is defined as

$$W = (C - C_o) + |(C - C_o)| \tag{5.9}$$

which again generates a positive value if the compliance is greater than the given value. With the above definitions, maximization of F in Eq.(5.7) will result in a reduction in the number of spot welds N and reduce the amount of the violations in S and W. Note that 1 is added to each of the terms in F (Eq.(5.7)) to avoid a zero denominator.

In addition to the problem formulation, several problem parameters are also important to the performance of the genetic algorithm. These parameters include the size of the population and the probabilities for various genetic manipulations. The size of the population is equal to the number of design candidates selected in one generation. Statistically, the problem with a larger population size has a better chance of obtaining a global optimal design than the problem with a smaller population size. However, this increased probability is achieved at the expense of more function

Reproduced with permission of the copyright owner. Further reproduction prohibited without permission.

evaluations. Thus, the selection of an appropriate population size is important. In this study, the population size used is approximately three times of the number of possible locations for spot welds. In regard to genetic manipulations, the probabilities are set at 100 percent for crossover and permutation, and at 10 percent for mutation in most of the examples.

Example 1

Two constrained components are welded together with 15 possible spot-weld locations, as shown in Fig. 5.5. A point load is applied to each of the components. Because the problem is symmetric, the optimum pattern of the spot welds is expected to be symmetric as well. In the formulation of S in Eq.(5.8), a_i is taken as the vector sum of the axial and shear forces at a spot weld, and a_o is taken as 17 units. Furthermore, the C_o in Eq.(5.9) is taken as 0.789 units.

The best three designs are shown in Figs. 5.6 to 5.8; these designs are obtained by using the genetic algorithm with 1357 function analyses. The best design has eight spot welds with an objective function of 0.0591 and a compliance of 0.792. The pattern of spot welds is symmetric. The end welds of the upper row sustain the highest reaction forces. The second best design has nine spot welds with an objective function of 0.0559. The pattern of spot welds is also symmetric. Its compliance is 0.790, which is slightly better than that of the best design. However, the design has one more spot weld than the best design. Again, the end welds of the upper row are subjected to the highest reaction forces. The third best design is not symmetric. It has eight spot welds with an objective function value of 0.0553. The maximum reaction force acts on the upper right corner of the pattern. Note that the magnitude of the maximum reaction force for the third best design is quite close to that of the best design.

Reproduced with permission of the copyright owner. Further reproduction prohibited without permission.

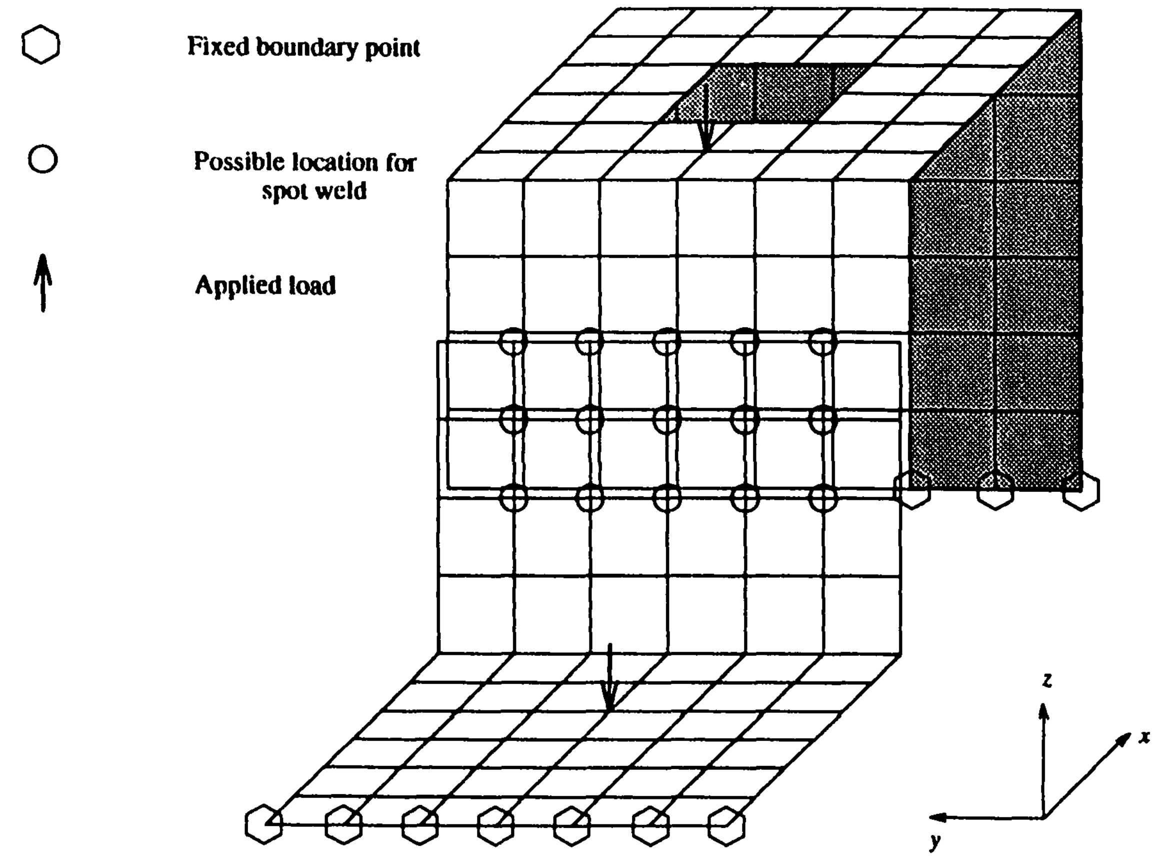

Figure 5.5. Model of two constrained components to be welded (example 1).

Reproduced with permission of the copyright owner. Further reproduction prohibited without permission.

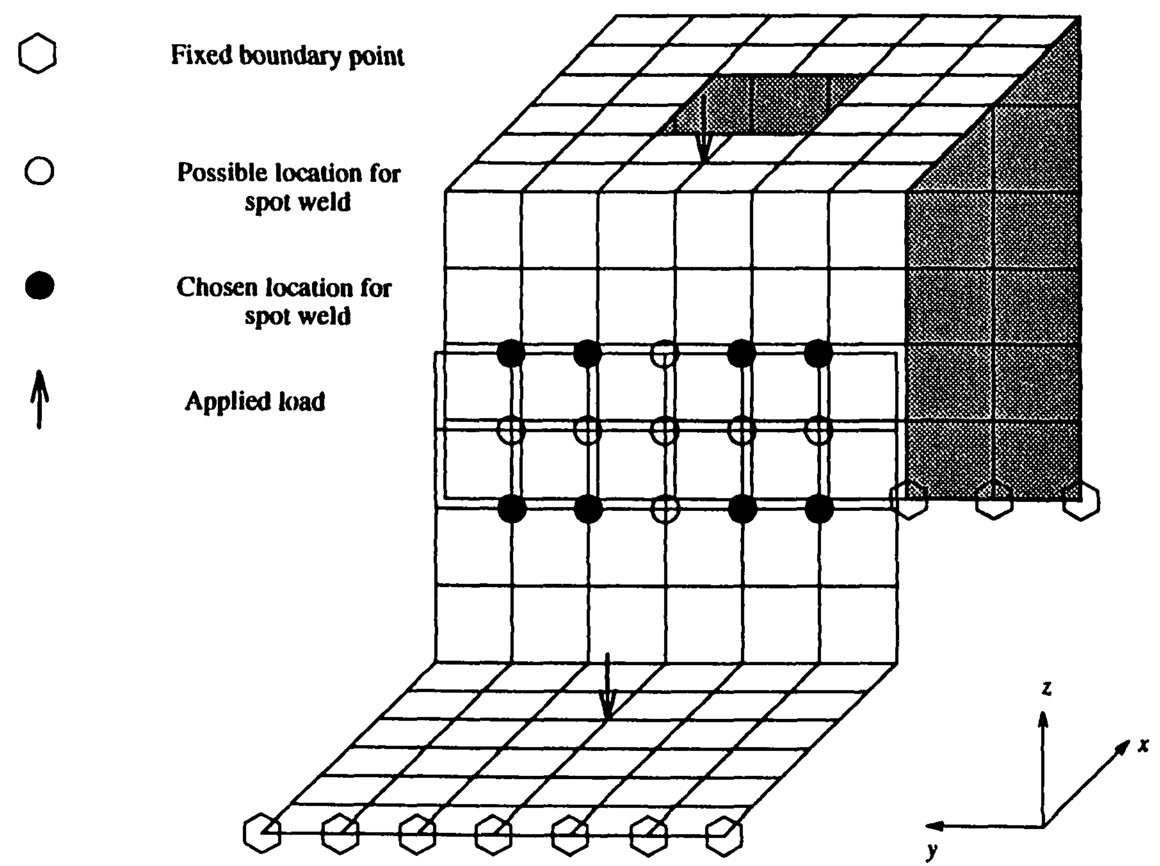

Figure 5.6. Best design for example 1.

Reproduced with permission of the copyright owner. Further reproduction prohibited without permission.

Reproduced with permission of the copyright owner. Further reproduction prohibited without permission.

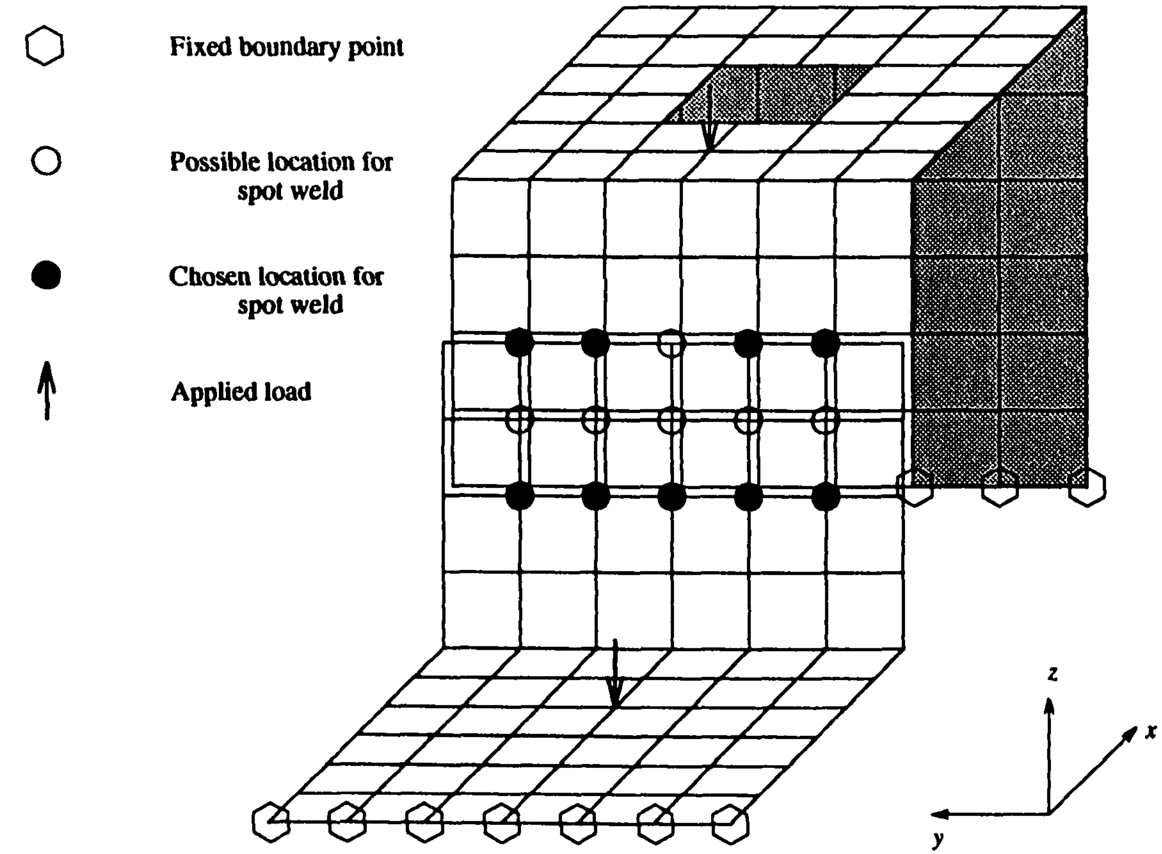

Figure 5.7. Second best design for example 1.

Reproduced with permission of the copyright owner. Further reproduction prohibited without permission.

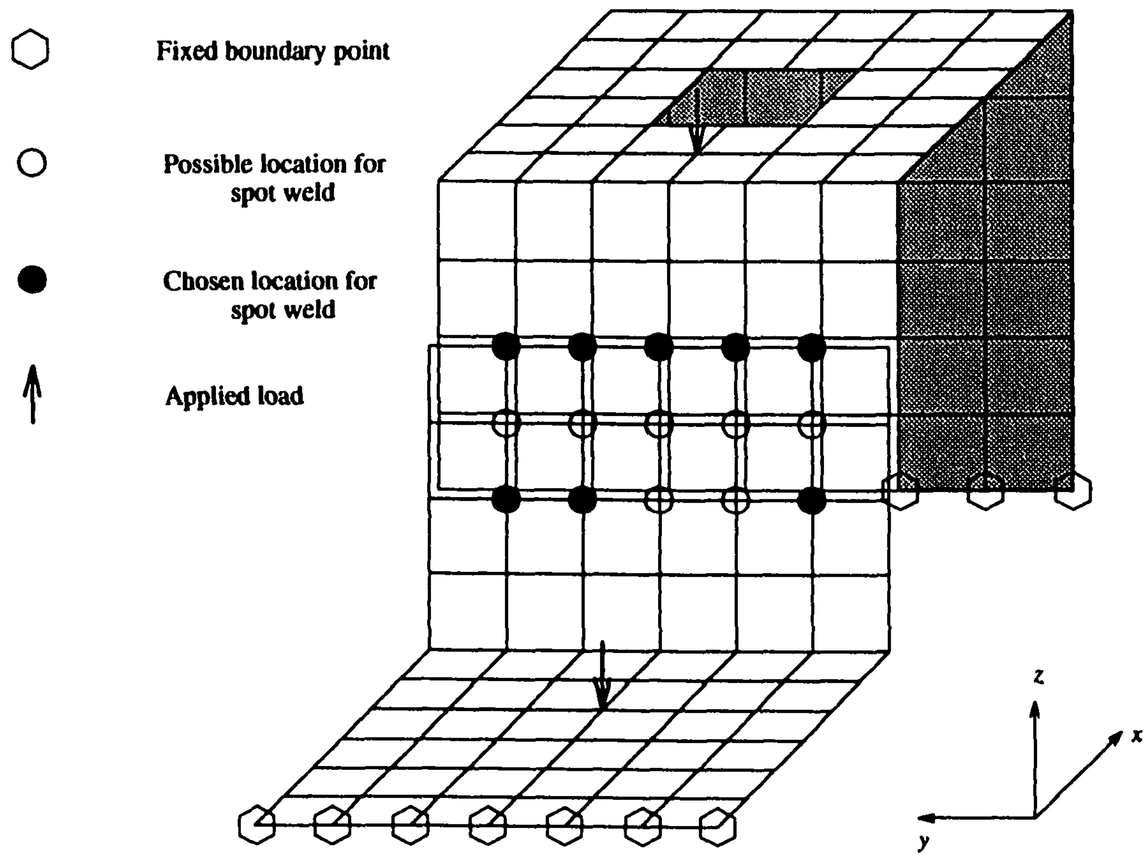

Figure 5.8. Third best design for example 1.

Example 2

A simpler model of the B pillar-to-rocket joint is used here. As shown in Fig. 5.9, six parts are spot welded together to assemble the B pillar-to-rocket joint. In this study, only a series of nine spot welds along the bottom edge that connect two parts are selected as the design variables. (See Fig. 5.10.) Both sides of the joint are fully constrained, and three point moments are applied at the open end of the joint. The problem formulation is the same as the formulation defined by Eqs.(5.7) through (5.9), except that the W term is multiplied by 10^6 in this example to ensure that the three terms in the denominator of Eq.(5.7) have an equal order of magnitudes.

A total of 725 function evaluations are necessary to reach the best designs. The constraint of S considers only the axial and shear forces in the spot welds, in which a_o is taken as one unit. The C_o here is 0.58115×10^{-4}. The best three designs are shown in Figs. 5.11 through 5.13. Because the structure of the B pillar-to-rocket joint is not symmetric, the solution is not expected to be symmetric. However, the best designs have only one or two spot welds. This surprising result demonstrates the importance of selecting the proper parameters in Eqs.(5.7) through (5.9) for design optimization. The three best designs shown here violate the compliance constraint described by Eq.(5.9). Furthermore, the second and third designs also violate the weld-strength constraint in Eq.(5.8). In other words, the best design is selected because it requires the fewest spot welds. This result is a direct consequence of the formulation of the merit function in Eq.(5.7), which implicitly places more weight on the number of the spot welds than on the strength of the welds and the magnitude of the compliance. A suggestion for overcoming this difficulty is to assign weighting coefficients to the factors in Eq.(5.7) as

$$F = 1/\{(\alpha N + 1)(\beta S + 1)(\gamma W + 1)\} \tag{5.10}$$

where the values α, β, and γ, along with the proper selection of C_o and a_o in Eqs.(5.8)

Reproduced with permission of the copyright owner. Further reproduction prohibited without permission.

and (5.9), will yield a design formulation that leads to more realistic designs. For example, if α is changed from 1 to 0.01, then the above problem yields an optimal design with eight spot welds, as shown in Fig. 5.14.

In conclusion, the proposed algorithm has been successfully implemented and demonstrated with two sample problems. The results show that the proposed algorithm can be used effectively to generate near-optimal patterns for spot welding. The results also reveal that the algorithm is sensitive to the parameters used in the problem formulation, such as α, β, γ, and a_0. Thus, research efforts are needed to provide general guidelines for the selection of these problem parameters in order to make the proposed algorithm a practical design tool.

Reproduced with permission of the copyright owner. Further reproduction prohibited without permission.

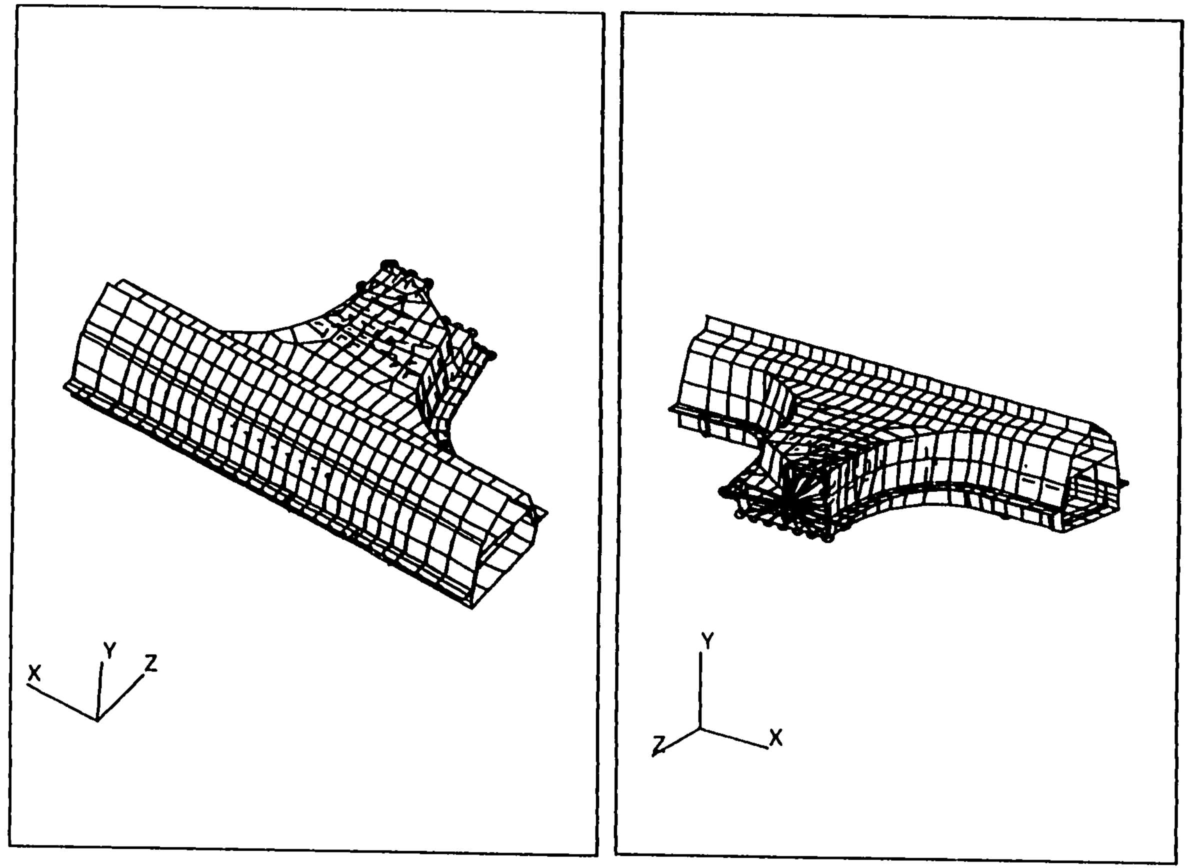

Figure 5.9. Finite-element model of B pillar-to-rocket joint.

Reproduced with permission of the copyright owner. Further reproduction prohibited without permission.

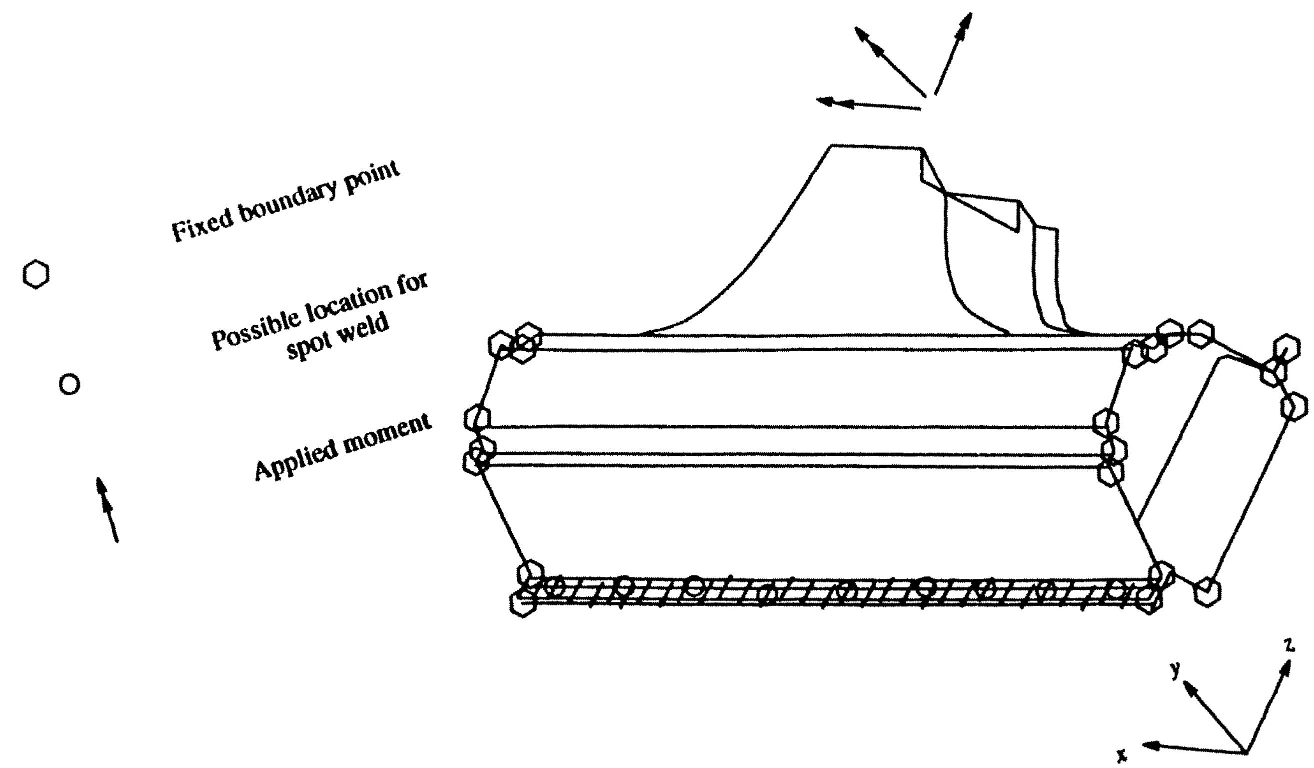

Figure 5.10. Model of B pillar-to-rocket joint (example 2).

Reproduced with permission of the copyright owner. Further reproduction prohibited without permission.

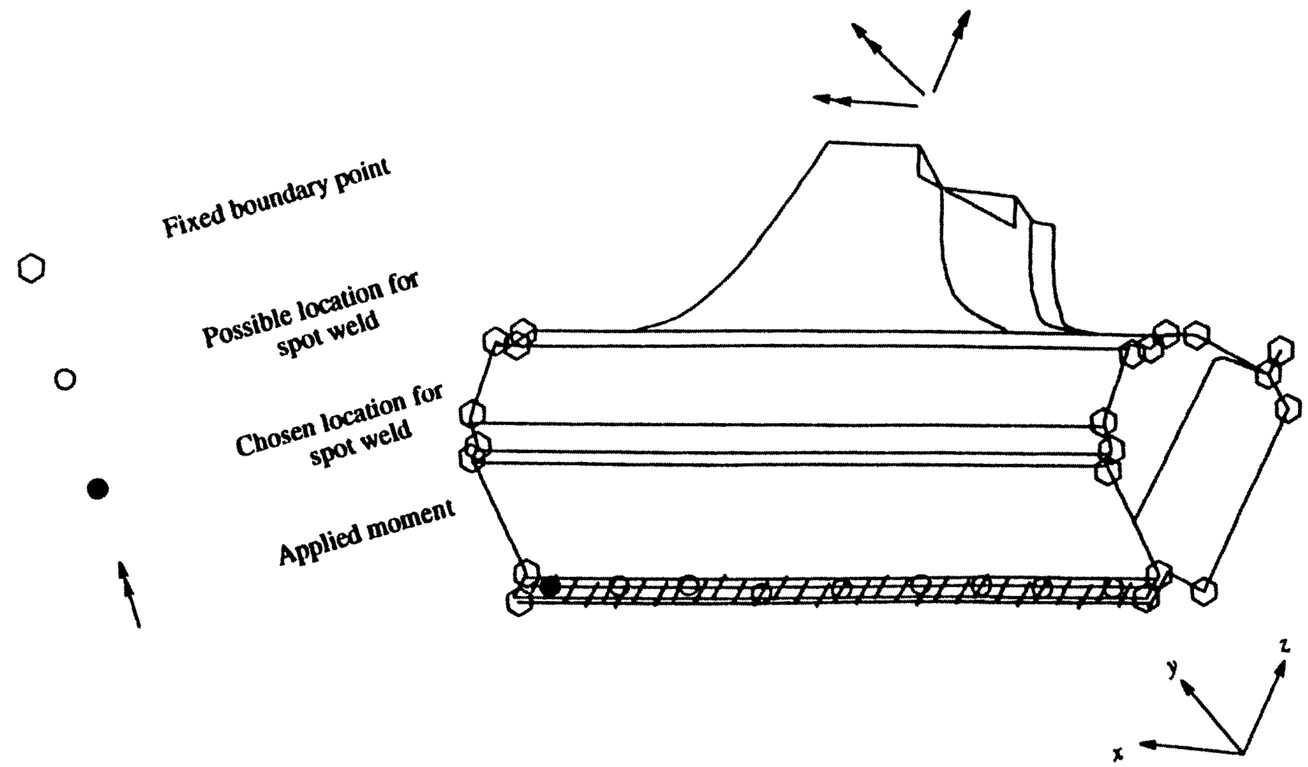

Figure 5.11. Best design for example 2.

Reproduced with permission of the copyright owner. Further reproduction prohibited without permission.

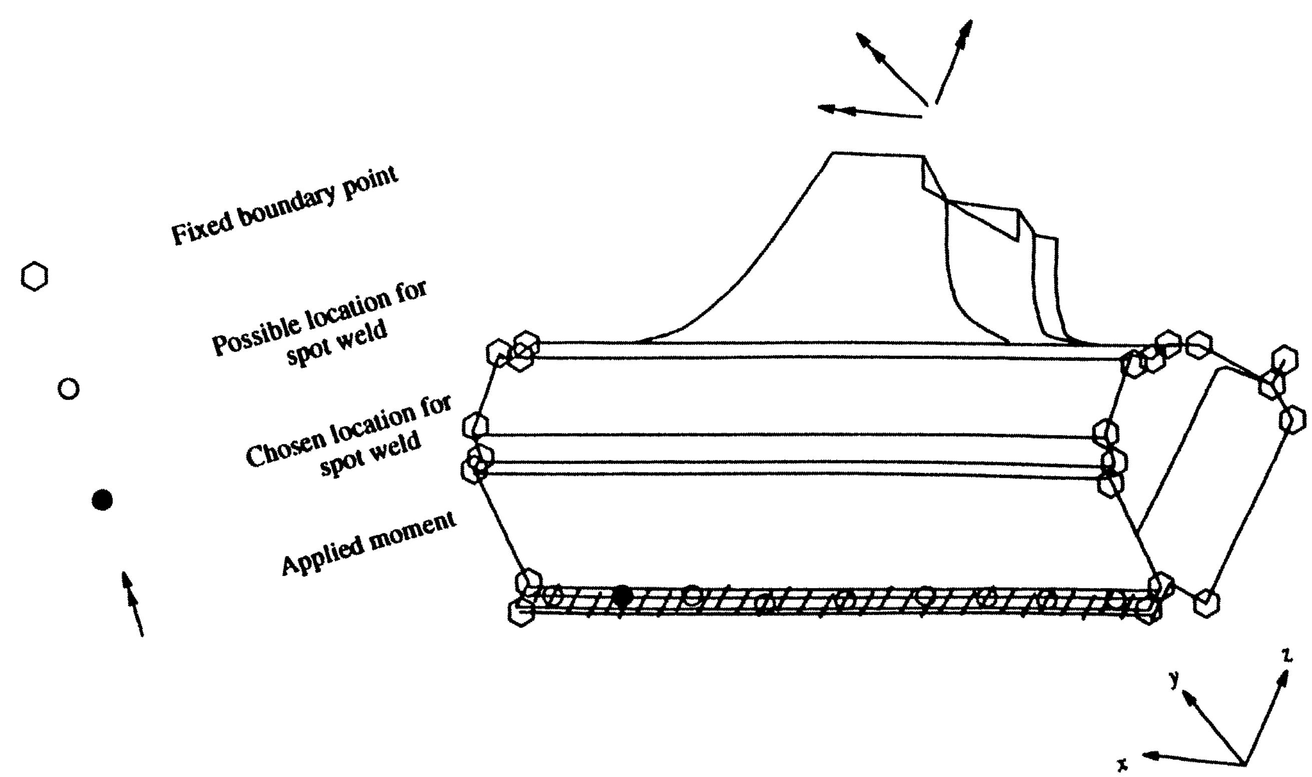

Figure 5.12. Second best design for example 2.

Reproduced with permission of the copyright owner. Further reproduction prohibited without permission.

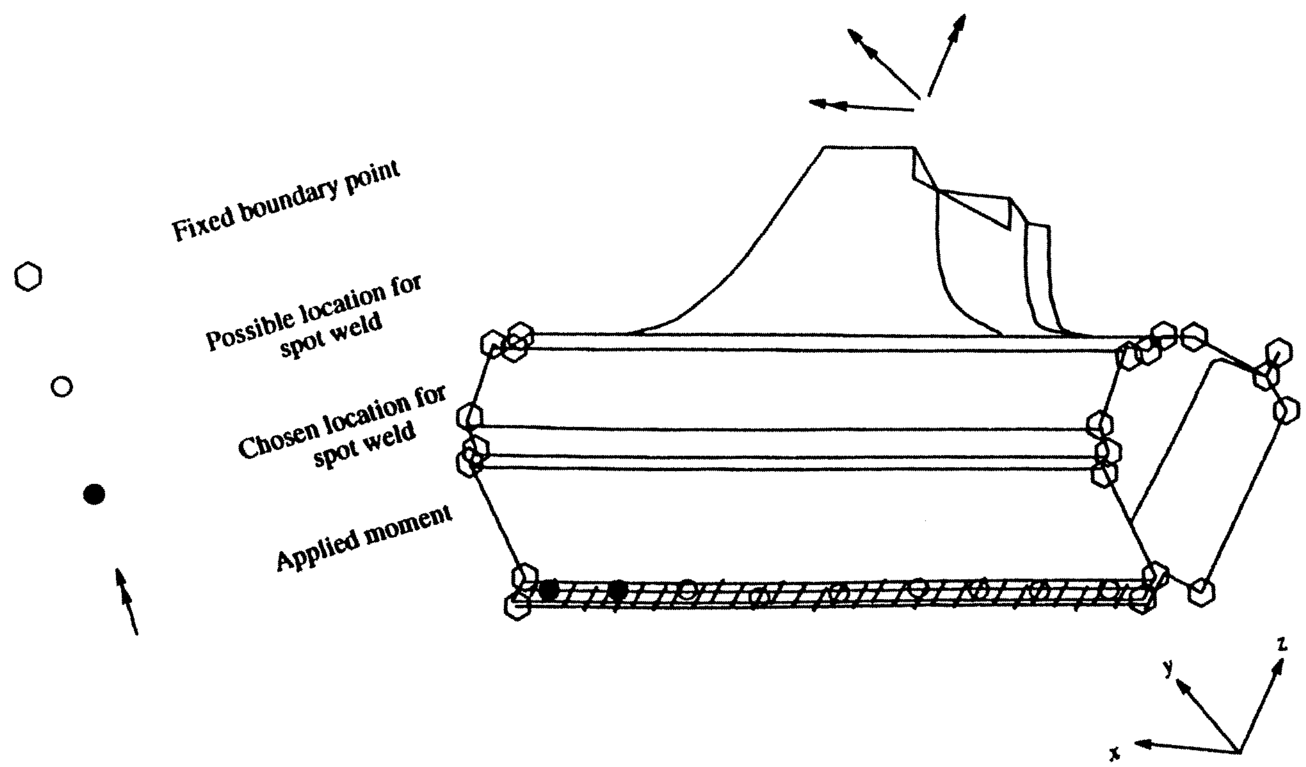

Figure 5.13. Third best design for example 2.

Reproduced with permission of the copyright owner. Further reproduction prohibited without permission.

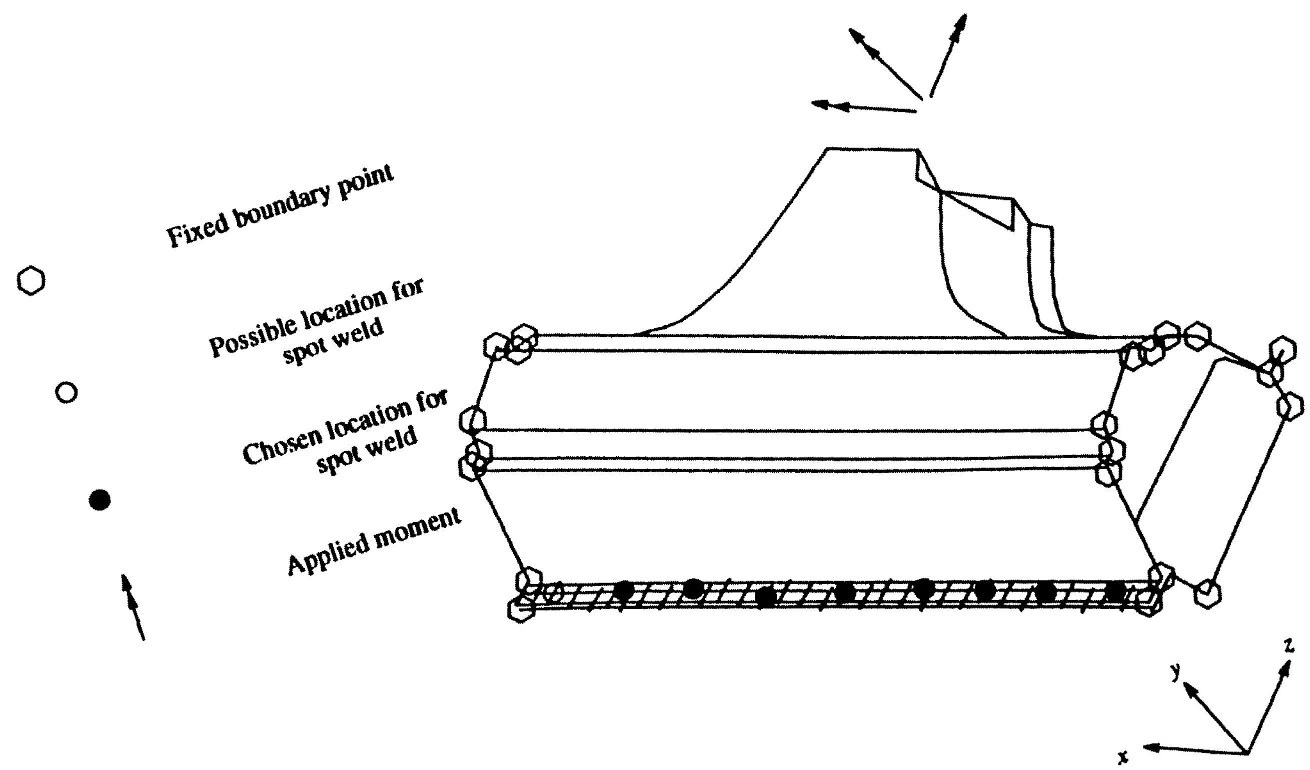

Figure 5.14. Best design for alternate objective function.

Reproduced with permission of the copyright owner. Further reproduction prohibited without permission.

CHAPTER 6

CONCLUDING REMARKS

The main thrust of this research was to develop a framework for a numerical approach for the optimal pattern design of spot welds and to assess this applicability of the approach in an industrial environment.

The pattern design of spot welds in this study is viewed as a combinatory design-optimization problem and solved by a genetic-algorithm-based search method incorporated with an efficient reanalysis technique. The reanalysis technique models the spot welds as multiple-point constraints and uses the Sherman-Morrison identity to recursively calculate the new solution of the structure, subjected to modification of the joint and support conditions. Simple examples are provided to validate and evaluate the method. The proposed computational procedure has a major advantage for reanalysis; because this procedure does not involve any modification of the stiffness matrix, it can be conveniently interfaced with any commercially rated finite-element analysis code.

The most difficult part of the proposed approach for optimum spot-weld patterning is the mathematical formulation of the problem to properly measure the quality of patterns of spot welds. This study focuses on three performance criteria: maximizing the rigidity of the welded structure, minimizing the number of spot welds, and maintaining satisfactory strength requirements in spot welds. These criteria are blended into a single merit function, with weighting coefficients assigned to each. The genetic algorithm then uses the merit functions of different designs as a guideline to produce offspring and, eventually, better designs.

Reproduced with permission of the copyright owner. Further reproduction prohibited without permission.

In this study, the rigidity of the welded structure and the strength of the spot welds are represented, respectively, by the compliance of the welded structure and the magnitude of internal forces in the welds. The representation of the rigidity by compliance is an acceptable practice. However, because the characteristics of the materials that surround the spot weld are changed in spot welding, internal forces alone cannot sufficiently represent the strength of the spot welds. A better model than the one used in this study is needed to calculate the strength of the spot welds.

The proposed algorithm has been successfully implemented and demonstrated with two sample problems. The results show that the proposed algorithm can be used effectively to generate near-optimal patterns for spot welding. The results also reveal that the algorithm is sensitive to parameters used in the problem formulation, such as α, β, γ, and a_o. Thus, research efforts are now needed to provide general guidelines for the selection of these problem parameters in order to make the proposed algorithm a practical design tool.

Finally, the success of the proposed research has demonstrated a new application of the Sherman-Morrison identity for efficient reanalysis of a structure under modifications of joint and support conditions. This research may ultimately lead to the discovery of additional applications of the Sherman-Morrison identity in structural reanalysis.

Reproduced with permission of the copyright owner. Further reproduction prohibited without permission.

REFERENCES

1. Kron, G., "A Set of Principles to Interconnect the Solutions of Physical Systems," *J. Appl. Phys.*, Vol. 24, 1953, pp. 965–980.

2. Dorr, M. R., *Domain Decomposion via Lagrange Multipliers*, UCRL-98532, Lawrence Livermore National Laboratory, 1988.

3. Farhat, C., and Geradin, M., "Using a Reduced Number of Lagrange Multipliers for Assembling Parallel Incomplete Field Finite Element Approximations," *Computer Methods in Applied Mechanics and Engineering*, Vol. 97, 1992, pp. 333–354.

4. Dávila, C. G., Ransom, J. B., and Aminpour, M. A., *Cross-Surface Interface Element for Coupling Built-up Structural Subdomains*, NASA Technical Memorandum 109125, July 1994.

5. Ransom, J. B., McCleary, S. L., and Aminpour, M. A., "A New Interface Element for Connecting Independently Modeled Substructures," AIAA Paper No. 93–1503, Apr. 1993.

6. Farhat, C., and Roux, F. X., "A Method of Finite Element Tearing and Interconnecting and its Parallel Solution Algorithm," *Internat. J. Numer. Methods Engrg.*, Vol. 32, 1991, pp. 1205–1227.

7. Arora, J. S., "Survey of Structural Reanalysis Techniques," *J. Struct. Div., ASCE*, Vol. 102, No. ST4, Proc. Paper 12056, Apr. 1976, pp. 783–802.

8. Argyris, J. H., and Kelsey, S., "Initial Strains in the Matrix Force Method of Structural Analysis," *Journal of the Royal Aeronautical Society*, Vol. 64, No. 596, Aug. 1960, pp. 493–495.

9. Argyris, J. H., Kelsey, S., and Grzedzielski, A. L. M., "The Discussion on the Initial Strain Concept," *Journal of the Royal Aeronautical Society*, Vol. 65, Feb. 1961, pp. 127–137.

10. Sobieszczanski, J., "Matrix Algorithm for Structural Modification Based on Parallel Element Concept," *American Institute of Aeronautics and Astronautics Journal*, Vol. 7, No. 11, Nov. 1969, pp. 2132–2139.

Reproduced with permission of the copyright owner. Further reproduction prohibited without permission.

11. Guan, D., and Zhang, X., "Modified Designs and Modified Computations," *Computers & Structures*, Vol. 49, No. 6, 1993, pp. 905–911.

12. Argyris, J. H., Brönlund, O. E., Roy, J. R., and Scharpf, D. W., "A Direct Modification Procedure for Displacement Method," *American Institute of Aeronautics and Astronautics Journal*, Vol. 9, No. 9, Sep. 1971, pp. 1861–1864.

13. Kavlie, D., and Powell, G. H., "Efficient Reanalysis of Modified Structures," *J. Struct. Div., ASCE*, Vol. 97, No. ST1, Proc. Paper 7846, Jan. 1971, pp. 377–392.

14. Kirsch, U., and Rubinstein, M. F., "Reanalysis for Limited Structural Design Modifications," *J. Eng. Mech. Div., ASCE*, Vol. 98, No. EM1, Proc. Paper 8706, Feb. 1972, pp. 61–70.

15. Golub, G. H., and Van Loan, C. F., *Matrix Computations*, The Johns Hopkins University Press, Baltimore, 1989.

16. Haftka, R. T., Gürdal, Z., and Kamat, M. P., *Elements of Structural Optimization*, Kluwer Academic Publishers, 2nd Edition, Dordrecht, 1990.

17. Goldberg, D. E., *Genetic Algorithms in Search, Optimization, and Machine Learning*, Addison-Wesley Publishing Company, Inc., New York, 1989.

18. Sheppard, S. D., and Strange, M., "Fatigue Life Estimation in Resistance Spot Welds," *Fatigue & Fracture of Engineering Materials & Structures*, Vol. 15, No. 6, Jun. 1992, pp. 531–550.

19. Lindberg, R. A., and Braton, N. R., *Welding and Other Joining Processes*, Allyn and Bacon, Boston, 1976.

20. Gourd, L. M., *Principles of Welding Technology*, Edward Arnold (Publishers) Ltd, London, 1980.

Reproduced with permission of the copyright owner. Further reproduction prohibited without permission.